JOURNAL OF COMPUTATIONAL PHYSICS 69, 283–324 (1987)

# Asymptotic Solutions of Numerical Transport Problems in Optically Thick, Diffusive Regimes

EDWARD W. LARSEN, J. E. MOREL, AND WARREN F. MILLER, JR.

*University of California, Los Alamos National Laboratory, Radiation Transport Group, X-6, Los Alamos, New Mexico 87545*

Received January 15, 1986; revised May 2, 1986

We present an asymptotic analysis of spatial differencing schemes for the discrete-ordinates equations, for diffusive media with spatial cells that are not optically thin. Our theoretical tool is an asymptotic expansion that has previously been used to describe the transition from analytic transport to analytic diffusion theory for such media. To introduce this expansion and its physical rationale, we first describe it for the analytic discrete-ordinates equations. Then, we apply the expansion to the spatially discretized discrete-ordinates equations, with the spatial mesh scaled in either of two physically relevant ways such that the optical thickness of the spatial cells is not small. If the result of either expansion is a legitimate diffusion description for either the cell-average or cell-edge fluxes, then we say that the appropriate flux has the appropriate diffusion limit; otherwise, we say it does not. We consider several transport differencing schemes that are applicable in neutron transport and thermal radiation applications. We also include numerical results which demonstrate the validity of our theory and show that differencing schemes that do have a particular diffusion limit are substantially more accurate, in the regime described by the limit, than those that do not. 

## I. INTRODUCTION

In considering deterministic numerical methods for neutron transport and radiative transfer problems, one often faces the situation that, due to computer memory or running time limitations, the spatial cells in at least some of the energy or frequency groups are optically thick. Since standard error analyses of numerical transport schemes generally predict errors that are small for optically thin cells and that grow with some power of the optical thickness [1–4], there is strong reason to question the accuracy of numerical results that are obtained for optically thick meshes.

However, for many applications, the problems in which optically thick cells occur are also ones for which the problem is "diffusive." We shall precisely define this term below, but for now, this roughly means that the solution of a diffusion equation is a good approximation to the solution of the transport equation. In the last decade, the mathematical relationship between transport and diffusion theory has been clarified in a large body of work showing that transport theory transitions into diffusion theory in a certain asymptotic limit. A sampling of this work is given



0021-9991/87 $3.00

in [5–9] ([8] is a review article). In the present article, we apply this same asymptotic expansion to the discretized transport equation, with an optically thick mesh, to determine whether a discretized version of the correct diffusion equation results. If it does, and if the spatial mesh is adequate for the discretized diffusion equation, then good numerical results should be expected; otherwise, they should not.

In the remainder of this introduction, we describe this idea in greater detail and give a summary of the rest of the article, where the idea is worked out fully and tested numerically. Since most of the earlier work relating transport and diffusion theory used the neutron transport equation as its point of departure, we use that equation with its corresponding nomenclature throughout this article. To keep the discussion simple, we restrict our analysis to the one-group discrete-ordinates equations in slab geometry. These equations specifically model one-group neutron transport and grey radiative transfer.

First, we discuss the nature of the asymptotic expansion, as applied to the analytic discrete-ordinates equations. This expansion applies to "diffusive" problems, by which we mean that three key assumptions hold:

(1) the physical medium is many mean free paths thick (i.e., is "optically thick");

(2) the collision process is scattering-dominated (i.e., absorption cross-sections are small);

(3) the angular flux, cross-sections, and source are continuous and vary spatially by, at most, a small amount over the distance of a mean free path.

The earlier work shows that, by writing the transport equation in dimensionless form and invoking these assumptions, one obtains:

$$\mu \frac{\partial \psi}{\partial x}(x, \mu) + \frac{\sigma_T(x)}{\varepsilon} \psi(x, \mu) = \left[ \frac{\sigma_T(x)}{\varepsilon} - \varepsilon \sigma_a(x) \right] \frac{1}{2} \int_{-1}^{1} \psi(x, \mu')\, d\mu' + \varepsilon Q(x). \tag{1.1}$$

Here $\sigma_T$, $\sigma_a$, $Q$ and $\psi$ are scaled versions of the total and absorption cross sections, source, and angular flux, and all quantities are $O(1)$ and have $O(1)$ derivatives with respect to $x$, except for the small parameter $\varepsilon$, which depends on the particular characteristics of the transport problem. Then, constructing an asymptotic solution of this equation for $\varepsilon \ll 1$, one obtains:

$$\psi(x, \mu) = \phi(x) + O(\varepsilon), \tag{1.2}$$

where

$$-\frac{d}{dx} \frac{1}{3\sigma_T(x)} \frac{d}{dx} \phi(x) + \sigma_a(x)\, \phi(x) = Q(x). \tag{1.3}$$

Thus, for diffusive transport problems in which Eq. (1.1) is a legitimate formulation, $\psi$ is well approximated by $\phi$, the solution of the diffusion equation (1.3).

In regions of any physical problem where the above three assumptions do not hold, and hence where Eq. (1.1) is not valid, the results (1.2) and (1.3) do not follow. In particular, for an otherwise thick and diffusive problem, at material interfaces, or on outer boundaries with nonisotropic (incident) boundary conditions, the angular flux varies by an $O(1)$ amount over the distance of a mean free path, and one must add to the right side of Eq. (1.2) a "boundary-layer" solution. The construction and manipulation of such boundary layers is discussed fully in [5–9]. The analysis in this article deals specifically with regions of a thick, diffusive problem where the three assumptions in the above paragraph are valid, and we assume that if $O(1)$ boundary layers exist, then they are adequately resolved by a suitably fine mesh. We shall discuss the effects of $O(1)$ boundary layers later in our numerical results section.

To proceed, we consider the spatially discretized discrete-ordinates version of Eq. (1.1), with a fixed angular quadrature set and spatial cell widths denoted by $\Delta x$. Since $\sigma_T$, $\sigma_a$, and $Q$ are $O(1)$ and have $O(1)$ derivatives, then standard truncation-error analyses show that, to achieve accurate solutions by making the truncation error small, $\sigma_T \Delta x/\varepsilon$ must be small in Eq. (1.1) [5, 6], and {if the diffusion length $L = (3\sigma_T \sigma_a)^{-1/2}$ is a typical distance over which $\phi$ in Eq. (1.3) varies by an $O(1)$ amount} $\sqrt{3\sigma_T \sigma_a}\, \Delta x$ small in Eq. (1.3). In other words, truncation errors in the discretized transport equation are small when the spatial mesh is optically thin, and truncation errors in the discretized diffusion solution are small when the mesh is fine enough to resolve variations in the solution. Thus, for Eqs. (1.1) and (1.3), the constraints on the mesh for achieving a small transport truncation error are much more strict than those for achieving a small diffusion truncation error. This occurs even though Eq. (1.2) indicates that the transport and diffusion solutions are nearly identical.

It is, thus, reasonable to ask if, for diffusive media, a given transport discretization can produce accurate results when $\sigma_T \Delta x/\varepsilon$ is not small. In particular, if a mesh $\Delta x = O(1)$ is reasonable for differencing the diffusion equation, but $\sigma_T \Delta x/\varepsilon$ is large, can one obtain transport results with accuracy comparable to that of the diffusion results with this mesh? Or, if a mesh $\Delta x = O(\varepsilon)$ is small for diffusion differencing but $\sigma_T \Delta x/\varepsilon = O(1)$ is not small, will accurate transport results *then* be obtained?

These are essential questions because, for many applications in both neutronics and radiative transfer, computer memory and running time limitations prohibit the use of a mesh which is sufficiently fine that the transport truncation error is small. Moreover, these questions cannot be addressed by a standard truncation error analysis because such analyses are valid only for spatial cells that are optically thin and, consequently, for which the truncation error is small. Thus, at present, there exists no theoretical justification for the use of "coarse" spatial meshes in any type of transport calculation.

The purpose of this article is to propose such a justification for diffusive media.

Our primary tool is the asymptotic procedure that leads from Eq. (1.1) to Eqs. (1.2) and (1.3). In particular, we apply this procedure to *discretized* versions of Eq. (1.1). If application of this procedure yields a legitimate discretized diffusion equation, then good numerical accuracy can be expected in this regime provided the spatial mesh is adequate for the discretized diffusion equation and provided any nondiffusive transport regions, for example, near boundaries or interfaces, are resolved by a suitably fine mesh. Conversely, if the transport discretization does not limit to a legitimate diffusion discretization, then the use of an optically coarse mesh in a diffusive problem should lead to poor numerical results.

We consider several spatial differencing schemes that are applicable in neutron transport and thermal radiation applications. The class of schemes considered here have two unknown fluxes per cell and are built upon the use of cell-edge and cell-average fluxes. It is natural to ask whether each of these quantities has a correct diffusion discription in a diffusive problem. Also, there are two natural lengths in diffusive problems, a typical mean free path and a typical distance over which the angular flux varies by an $O(1)$ amount (a "scale length"). Thus, to obtain a reasonable discretized approximation of the transport equation for diffusive problems, it is natural to consider spatial meshes chosen such that the width of a spatial cell is comparable either to a scale length or to a mean free path. We denote these two regimes as "thick" and "intermediate," since these labels describe the optical thicknesses of the spatial cells in the two cases. (We add parenthetically that radiative transfer calculations characteristically use spatial meshes that are optically "thick," while neutronics calculations characteristically use spatial meshes that are optically "intermediate." "Thin" regimes, for which the optical thickness of the cells and the truncation error are small, can be treated by standard truncation error analyses, and will not be considered in this article. Thus, although certain practical problems of a diffusive nature do occur in media which are optically thin, these will not be analyzed here.)

Therefore, with two basic unknowns, the cell-average and cell-edge fluxes, and two chosen scalings for the spatial mesh, there are a total of four asymptotic limits for each differencing scheme. The schemes with two unknowns per cell that we consider in this article are the diamond-difference [10, 11], step [10, 11], Lund–Wilson [12, 13], and Castor [14] schemes, together with a "new" scheme. Our asymptotic analysis, described in Sections IV–VII, gives results that are summarized in Table I.

In this table, the term "maybe" indicates that for general problems in the indicated regime, the method does not have the indicated limit, but under special conditions the method does have the indicated limit. These special conditions are summarized in Table I and are fully discussed in Sections IV–VII.

The work presented in this article is based, in part, on earlier work which considered the behavior of transport differencing schemes in optically thick, diffusive media [12–17]. In particular, Grant [15] and Brown, Hill, and Pomraning [16] present criteria that are sufficient, but not necessary, for determining whether at least one correct diffusion limit exists. In [12–13], the Lund–Wilson method is

TABLE I

Summary of Results

| | Intermediate | | Thick | |
|---|---|---|---|---|
| | Edge | Average | Edge | Average |
| Diamond | yes | yes | maybe[a] | yes |
| Step | maybe[b] | maybe[b] | maybe[b] | maybe[b] |
| Lund–Wilson | no | maybe[b] | no | yes |
| Castor | no | maybe[c] | no | yes |
| New | yes | yes | yes | yes |

Qualifiers are defined as follows:

[a] Yes only if boundary sources are isotropic.

[b] Yes only if $\sigma_{aj} = Q_j = 0$ and $(\sigma_T h)_{j+1/2} = \text{constant}$.

[c] Yes only if $(\sigma_T h)_{j+1/2} = \text{constant}$.

presented as a positive differencing scheme which, for the cell-average fluxes, transitions to a cell-centered diffusion description as the optical thickness of the spatial cells becomes large. In [14], Castor's method is presented as a method which, for the cell-average fluxes, more accurately transitions to a cell-centered diffusion description for spatial cells of all optical thicknesses. Castor's theoretical tool is a Fourier analysis that requires $\sigma_T$, $\sigma_a$, and $\Delta x$ to be constant; the asymptotic analysis in this article does not inherently require such assumptions. Finally, in [17], Larsen employs an asymptotic expansion which is equivalent to the "intermediate" expansion used in this article, but no distinction is made between diffusion limits for cell-average and cell-edge fluxes. The present article draws from all this prior work and attempts to combine, clarify, and complete it.

An outline of the remainder of this article follows. In Section II we introduce notation and motivate the concepts underlying the asymptotic analysis by casting the analytic slab geometry discrete-ordinates equations into dimensionless form and carrying out this asymptotic analysis to derive analytic diffusion theory. In Section III we discuss two key items: the application of the asymptotic analysis to the spatially discretized discrete-ordinates equations, and two physically motivated scalings for the spatial mesh. We carry out the asymptotic analysis in Section IV for the diamond-difference method [10, 11], in Section V for the step method [10, 11], in Section VI for the Lund–Wilson [12, 13] and Castor [14] methods, and in Section VII for the "new" method. In Section VIII, we present numerical results that test and confirm the predictions made in Sections IV–VII, and we conclude with a brief discussion in Section IX.

## II. Asymptotic Analysis of the Analytic Discrete-Ordinates Equations

In this section we consider the steady, monoenergetic, discrete-ordinates equations with isotropic scattering,

$$\mu_m \frac{d\tilde{\psi}_m}{dz}(z) + \tilde{\sigma}_T(z)\,\tilde{\psi}_m(z) = \tilde{\sigma}_s(z) \sum_{n=1}^{N} \tilde{\psi}_n(z)\, w_n + \tilde{Q}(z), \qquad m = 1,..., N, \quad (2.1)$$

and the standard diffusion approximation to these equations,

$$-\frac{d}{dz}\frac{1}{3\tilde{\sigma}_T(z)}\frac{d}{dz}\tilde{\phi}(z) + \tilde{\sigma}_a(z)\,\tilde{\phi}(z) = \tilde{Q}(z), \quad (2.2)$$

where

$$\tilde{\sigma}_a(z) = \tilde{\sigma}_T(z) - \tilde{\sigma}_s(z). \quad (2.3)$$

The notation here is standard [10, 11], except for the tildes, which indicate dimensional quantities. In Eqs. (2.1), we employ an order-$N$ quadrature set $\{\mu_m, w_m | m = 1,..., N\}$ with weights $w_m$ normalized as

$$\sum_{n=1}^{N} w_n = 1. \quad (2.4)$$

Boundary conditions for Eqs. (2.1) and (2.2) will, for now, be unspecified.

Here we shall derive Eq. (2.2) from Eq. (2.1) using an asymptotic expansion. Our purpose is to establish notation, to derive the discrete-ordinates versions of the dimensionless Eqs. (1.1)–(1.3) from (2.1)–(2.3) so that the former equations can be used in place of the latter in succeeding sections, and to present the basic ideas underlying the asymptotic analysis.

To begin, we consider $\tilde{\sigma}_T(z)$, $\tilde{\sigma}_s(z)$, $\tilde{Q}(z)$, $\tilde{\psi}_m(z)$, and $\tilde{\phi}(z)$ in Eqs. (2.1) and (2.2) to all be continuous, smoothly varying functions of $z$, and we define a "scale length" $\rho$ for these quantities to be a typical distance over which they vary by, at most, an $O(1)$ amount. For one example, let $\tilde{Q}(z)$ be a delta function, let $\tilde{\sigma}_T$, $\tilde{\sigma}_s$ be constants with $0 < \tilde{\sigma}_s < \tilde{\sigma}_T$, and let us consider a region bounded away from the support of the delta function (i.e., bounded away from boundary layers). The diffusion length $L$, defined by

$$L = (3\tilde{\sigma}_T\,\tilde{\sigma}_a)^{-1/2}, \quad (2.5)$$

would be a reasonable choice for $\rho$ since $\tilde{\phi}$ (and, approximately, $\tilde{\psi}$) will undergo a relative $O(1)$ change over this distance in this region. For another example, let $\tilde{\sigma}_T = \tilde{\sigma}_s$ be constants, $\tilde{Q}$ be a positive constant, and the system be a finite slab of thickness $X$ with vacuum boundary conditions. Then, $\tilde{\psi}_m$ and $\tilde{\phi}$ will be roughly parabolic in shape, with the approximate value of zero at the edges of the system and having maxima at the center of the system. Here an appropriate choice for $\rho$ is

not the diffusion length, which has the value $L = \infty$, but rather $\rho = X/2$. In general, the definition of $\rho$ is not precise, but is indicated by the special nature of the problem under consideration. Henceforth, we shall assume that a particular problem is in mind, and for this problem, one can select an appropriate scale length $\rho$.

Let us now define a new dimensionless distance variable $x$ in terms of $z$ and the scale length $\rho$ by

$$x = z/\rho, \tag{2.6}$$

and let us introduce

$$\psi_m(x) = \tilde{\psi}_m(z), \tag{2.7a}$$

$$\phi(x) = \tilde{\phi}(z). \tag{2.7b}$$

Then $\psi_m$ and $\phi$ vary by, at most, an $O(1)$ amount over an $O(1)$ distance in $x$, and we make the reasonable assumptions that in a diffusive region

$$\left(\frac{d}{dx}\right)^n \psi_m(x) = O(1), \qquad \left(\frac{d}{dx}\right)^n \phi(x) = O(1), \qquad n = 1,.... \tag{2.8}$$

(We note that these assumptions are reasonable only if the cross sections and source have the same scale length $\rho$, but this is assumed above in the definition of $\rho$.)

Using Eqs. (2.6) and (2.7), we can rewrite (2.1) and (2.2) as

$$\mu_m \frac{d\psi_m}{dx}(x) + \rho\tilde{\sigma}_T(z)\,\psi_m(x) = \rho\tilde{\sigma}_s(z) \sum_{n=1}^{N} \psi_n(x)\, w_n + \rho\tilde{Q}(z), \tag{2.9}$$

$$-\frac{d}{dx}\frac{1}{3\rho\tilde{\sigma}_T(z)}\frac{d}{dx}\phi(x) + \rho\tilde{\sigma}_a(z)\,\phi(x) = \rho\tilde{Q}(z). \tag{2.10}$$

Next, we let $\langle\tilde{\sigma}_T\rangle$ be a typical value of $\tilde{\sigma}_T(z)$, and we define

$$\sigma_T(x) = \frac{\tilde{\sigma}_T(z)}{\langle\tilde{\sigma}_T\rangle}; \tag{2.11}$$

then $\sigma_T(x) = O(1)$. We may write

$$\rho\tilde{\sigma}_T(z) = \rho\langle\tilde{\sigma}_T\rangle\,\sigma_T(x) = \frac{1}{\varepsilon}\sigma_T(x), \tag{2.12}$$

where

$$\varepsilon = \frac{1}{\rho\langle\tilde{\sigma}_T\rangle} = \frac{\text{typical mean free path}}{\text{scale length}}, \tag{2.13}$$

and Eqs. (2.9) and (2.10) become

$$\mu_m \frac{d}{dx}\psi_m(x) + \frac{\sigma_T(x)}{\varepsilon}\psi_m(x) = \rho\tilde{\sigma}_s(z)\sum_{n=1}^{N}\psi_n(x)\,w_n + \rho\tilde{Q}(z), \quad (2.14)$$

$$-\frac{d}{dx}\frac{\varepsilon}{3\sigma_T(x)}\frac{d}{dx}\phi(x) + \rho\tilde{\sigma}_a(z)\,\phi(x) = \rho\tilde{Q}(z). \quad (2.15)$$

Now we consider the three assumptions stated in the first paragraph of the Introduction. In particular, we shall mathematically formulate these assumptions in such a way that Eq. (2.15) can be asymptotically derived from Eq. (2.14).

First, the assumptions that $\psi$ varies by a small amount over the distance of a mean free path and by an $O(1)$ amount over a scale length imply that there must be many mean free paths in a scale length. Thus, Eq. (2.13) gives

$$\varepsilon \ll 1. \quad (2.16)$$

The assumption that the system is optically thick is met by requiring the system to be comparable to (or larger than) a scale length. Also, if we set

$$\rho\tilde{\sigma}_a(z) = \varepsilon\sigma_a(x), \quad (2.17)$$

where $\sigma_a$ is $O(1)$, then absorptions are small and, as seems desirable, the leakage and absorption terms on the left side of Eq. (2.15) are comparable in size. Likewise, we set

$$\rho\tilde{Q}(z) = \varepsilon Q(x), \quad (2.18)$$

so that all the terms in Eq. (2.15) are comparable in size. Then, since $\varepsilon$ divides out of this equation, $\phi$ will be $O(1)$ with respect to $\varepsilon$, and if $\psi \approx \phi$, $\psi$ will be $O(1)$ also. The scaling (2.18) is not essential because multiplication of $\varepsilon Q$ by any other power of $\varepsilon$ will merely result in a multiplication of the solutions ($\psi$ and $\phi$) by the same power of $\varepsilon$. However, the scaling (2.18) is convenient, and hence we shall use it.

Now, combining Eqs. (2.14)–(2.18) and (2.3), we obtain

$$\mu_m\frac{d\psi_m}{dx} + \frac{\sigma_T}{\varepsilon}\psi_m = \left(\frac{\sigma_T}{\varepsilon} - \varepsilon\sigma_a\right)\sum_{n=1}^{N}\psi_n w_n + \varepsilon Q, \quad (2.19)$$

$$-\frac{d}{dx}\frac{1}{3\sigma_T}\frac{d}{dx}\phi + \sigma_a\phi = Q, \quad (2.20)$$

which are just Eqs. (1.3) and (the discrete-ordinates version of) (1.1). These dimensionless equations are equivalent to the dimensional equations (2.1) and (2.2), and the three assumptions discussed above Eq. (1.1) are equivalent to the requirements that $\psi_m$, $\sigma_T$, $\sigma_a$, and $Q$ are $O(1)$ and have $O(1)$ derivatives with respect to $x$, and that $\varepsilon \ll 1$.

To derive Eq. (2.20) from Eq. (2.19), we introduce the ansatz,

$$\psi_m(x) \approx \sum_{k=0}^{\infty} \varepsilon^k \psi_m^{(k)}(x), \tag{2.21}$$

into Eq. (2.19) and equate the coefficients of different powers of $\varepsilon$ to obtain the system of equations

$$\sigma_T \left[ \psi_m^{(k)} - \sum_{n=1}^{N} \psi_n^{(k)} w_n \right] = -\mu_m \frac{d\psi_m^{(k-1)}}{dx} - \sigma_a \sum_{n=1}^{N} \psi_n^{(k-2)} w_n + \delta_{k2} Q, \qquad k = 0, 1, 2, \ldots, \tag{2.22}$$

with $\psi^{(-1)} = \psi^{(-2)} = 0$. We now solve these equations recursively.

Equation (2.22) with $k = 0$ is

$$\sigma_T \left[ \psi_m^{(0)} - \sum_{n=1}^{N} \psi_n^{(0)} w_n \right] = 0, \tag{2.23}$$

which, because of the normalization (2.4), implies

$$\psi_m^{(0)}(x) = \phi^{(0)}(x), \tag{2.24}$$

where $\phi^{(0)}(x)$ is, for now, undetermined.

Equation (2.22) with $k = 1$ is

$$\sigma_T \left[ \psi_m^{(1)} - \sum_{n=1}^{N} \psi_n^{(1)} w_n \right] = -\mu_m \frac{d\phi^{(0)}}{dx}. \tag{2.25}$$

In order that a solution $\psi_m^{(1)}$ of this equation exist, a solvability condition must be met. Namely, if we multiply by $w_m$ and sum over all $m$, the left side vanishes, and we obtain as a condition for the existence of $\psi_m^{(1)}$

$$0 = -\left( \sum_{n=1}^{N} \mu_n w_n \right) \frac{d\phi^{(0)}}{dx}, \tag{2.26}$$

which, to obtain a nonconstant $\phi^{(0)}$, requires

$$0 = \sum_{n=1}^{N} \mu_n w_n. \tag{2.27}$$

Assuming that this condition on the quadrature set is met, we obtain as the general solution of Eq. (2.25)

$$\psi_m^{(1)} = \phi^{(1)} - \frac{\mu_m}{\sigma_T} \frac{d\phi^{(0)}}{dx}, \tag{2.28}$$

where $\phi^{(1)}$ is undetermined.

Equation (2.22) with $k=2$ is

$$\sigma_T\left[\psi_m^{(2)}-\sum_{n=1}^{N}\psi_n^{(2)}w_n\right]=-\mu_m\frac{d}{dx}\left(\phi^{(1)}-\frac{\mu_m}{\sigma_T}\frac{d\phi^{(0)}}{dx}\right)-\sigma_a\phi^{(0)}+Q, \tag{2.29}$$

and the solvability condition for this equation is

$$0=\left(\sum_{n=1}^{N}\mu_n^2 w_n\right)\frac{d}{dx}\frac{1}{\sigma_T}\frac{d}{dx}\phi^{(0)}-\sigma_a\phi^{(0)}+Q. \tag{2.30}$$

This is the standard diffusion equation, provided

$$\sum_{n=1}^{N}\mu_n^2 w_n=\frac{1}{3}. \tag{2.31}$$

Thus, if the constraints (2.27) and (2.31) on the quadrature set hold, then $\psi_m=\phi^{(0)}+0(\varepsilon)$, where $\phi^{(0)}$ satisfies Eq. (2.20). Equivalently, the connection between $\psi_m$ in Eq. (2.19) and $\phi$ in Eq. (2.20) is

$$\psi_m=\phi+O(\varepsilon). \tag{2.32}$$

This, of course, is just the discrete-ordinates version of Eq. (1.2).

The asymptotic analysis has shown several things. First, if the quadrature set "integrates" up to quadratic powers of $\mu_m$ correctly, then standard diffusion theory well-approximates transport theory in the asymptotic regime described above. In practice, quadrature sets are usually chosen to satisfy these constraints; and for the remainder of this article, we shall assume that the constraints hold. Second, the $O(1)$ component of $\psi_m$ is isotropic, and the $O(\varepsilon)$ component is linear in $\mu_m$. Third, the scalings (2.12), (2.17), and (2.18) have the following physical content: the probable number of collisions a particle undergoes in a scale length is large $[O(1/\varepsilon)]$, and is inversely proportional to two small $[O(\varepsilon)]$ quantities, the probable number of absorptions in a scale length, and the probable number of source particles emitted in a scale length.

## III. Asymptotic Scaling of the Spatially Discretized Discrete-Ordinates Equations

The starting point for the remaining analysis in this article is the balance equation, obtained by integrating Eq. (2.19) over the $j$th spatial cell $x_{j\,1/2}<x<x_{j+1/2}$:

$$\frac{\mu_m}{\Delta x_j}(\psi_{m,j+1/2}-\psi_{m,j-1/2})+\frac{\sigma_{Tj}}{\varepsilon}\psi_{mj}=\left(\frac{\sigma_{Tj}}{\varepsilon}-\varepsilon\sigma_{aj}\right)\sum_{n=1}^{N}\psi_{nj}\,w_n+\varepsilon Q_j. \tag{3.1}$$

Here, we have defined

$$\psi_{m,j+1/2} = \psi_m(x_{j+1/2}), \tag{3.2}$$

$$\psi_{mj} = \frac{1}{\Delta x_j} \int_{x_{j-1/2}}^{x_{j+1/2}} \psi_m(x)\, dx, \tag{3.3}$$

$$Q_j = \frac{1}{\Delta x_j} \int_{x_{j-1/2}}^{x_{j+1/2}} Q(x)\, dx, \tag{3.4}$$

$$\Delta x_j = x_{j+1/2} - x_{j-1/2}, \tag{3.5}$$

and we have taken $\sigma_{Tj}$ and $\sigma_{aj}$ to be representative values of $\sigma_T(x)$ and $\sigma_a(x)$ in the $j$th cell.

If, in the physical problem to solved, $\sigma_T$ and $\sigma_a$ are constant in the $j$th cell, then Eq. (3.1) is exact, in the sense that it follows without approximation from Eq. (2.19). However, it contains two basic unknowns, the cell-edge and cell-average fluxes, and an extra "auxiliary" equation relating these two fluxes must be specified so that the resulting two equations yield a viable numerical method. Various auxiliary equations are specified later in this article; here we discuss Eq. (3.1) and, in particular, our choice of scalings for $\Delta x_j$.

First, we note from Eq. (2.6) that

$$\frac{1}{\Delta x} = \frac{\rho}{\Delta z} = \text{ the number of spatial cells in a scale length.} \tag{3.6}$$

Thus, the largest reasonable value for $\Delta x$, from the point of view of mesh refinement, is $\Delta x = O(1)$. This means that, at most, a "few" spatial cells are available to resolve an $O(1)$ variation in $\psi$, and since

$$\tilde{\sigma}_T\, \Delta z = \frac{\sigma_T\, \Delta x}{\varepsilon} = O\left(\frac{1}{\varepsilon}\right), \tag{3.7}$$

then each spatial cell is many [i.e., $O(1/\varepsilon)$] mean free paths thick. We define this as the "thick" diffusion regime.

A second reasonable value for $\Delta x$ is $\Delta x = O(\varepsilon)$. This means that $O(1/\varepsilon)$ spatial cells are available to resolve an $O(1)$ variation in $\psi$, and that

$$\tilde{\sigma}_T\, \Delta z = \frac{\sigma_T\, \Delta x}{\varepsilon} = O(1), \tag{3.8}$$

so that each spatial cell is on the order of a mean free path thick. We define this as the "intermediate" diffusion regime.

Other possible scalings are $\Delta x = O(\varepsilon^l)$ for $l \geqslant 2$. Now $O(1/\varepsilon^l)$ spatial cells are available to resolve an $O(1)$ variation in $\psi$, and

$$\tilde{\sigma}_T\, \Delta z = O(\varepsilon^{l-1}), \tag{3.9}$$

so each cell is a very small fraction of a man free path thick. We describe this as the "thin" diffusion regime.

To summarize, if $h_j = O(1)$ and

$$\Delta x_j = \varepsilon^l h_j, \tag{3.10}$$

then the three regimes are defined by

$$l = \begin{cases} 0 & \text{thick} \\ 1 & \text{intermediate} \\ \geqslant 2 & \text{thin.} \end{cases} \tag{3.11}$$

Here, the name assigned to each regime connotes the optical thickness of a typical spatial cell.

In the remainder of this article, we shall dwell on the thick ($l=0$) and intermediate ($l=1$) regimes; here we simply state that all the discretization methods treated below have both the cell-average and cell-edge diffusion limits in the thin ($l \geqslant 2$) regime. (The proof of this lies in performing the "same" asymptotic analysis as we show for the $l=0$ and $l=1$ cases below.) This result is not unexpected because, in the thin regime, the mesh is scaled in such a way that as $\varepsilon \to 0$, the optical thickness of a cell, and hence the truncation error, both tend to zero; thus, the asymptotic analysis of the analytic transport equation applies. As stated in the Introduction, our main concern in this article is with regimes in which the optical thickness of the spatial cells (i.e., the formal truncation error) does not tend to zero.

To clarify the meaning of the thick and intermediate diffusion limits, let us consider Fig. 1. On this figure, the point labeled "Discretized $S_N$" denotes any problem with $\varepsilon > 0$ and $\Delta x > 0$. (See [18].) As $\Delta x \to 0$ with $\varepsilon$ fixed, the discretized $S_N$ equations converge to the analytic $S_N$ equations ($\Delta x = 0$, $\varepsilon > 0$), as shown in the figure. If now $\varepsilon \to 0$, the analytic $S_N$ equations converge to the analytic diffusion equation ($\Delta x = 0$, $\varepsilon = 0$), as is shown in the figure, and as we proved in Section 2.

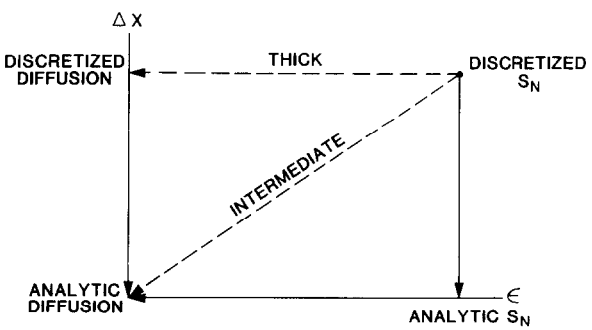


FIG. 1. Comparison of the thick and intermediate diffusion limits.

Also, if one starts with a legitimate discretized diffusion equation (labeled as $\Delta x > 0$, $\varepsilon = 0$), and lets $\Delta x \to 0$, one obtains the analytic diffusion equation, as shown in the figure.

In the thick diffusion regime, we have $\Delta x = h = O(1)$; thus, as $\varepsilon \to 0$, we (in principle) move along the horizontal dashed line linking "Discretized $S_N$" to "Discretized Diffusion." If, upon calculating this limit, the cell-average (or cell-edge) fluxes, in fact, are determined by a "legitimate" discretized diffusion equation, then we say that the cell-average (or cell-edge) fluxes have the thick diffusion limit; otherwise, we say they do not. (By "legitimate," we mean that as $\Delta x \to 0$, the correct analytic diffusion equation results.)

In the intermediate diffusion regime we have $\Delta x = \varepsilon h$, and thus as $\varepsilon \to 0$, we, in principle, move along the diagonal dashed line linking "Discretized $S_N$" to "Analytic Diffusion." [Note that the slope of this line is $h$, hence is $O(1)$.] If, upon calculating this limit, the cell-average (or cell-edge) fluxes, in fact, are determined by the analytic diffusion equation, then we say that the cell-average (or cell-edge) fluxes possess the intermediate diffusion limit; otherwise, we say they do not.

For any specific discretized $S_N$ problem, one can determine numerical values for the dimensionless quantities $\varepsilon$ [Eq. (2.13)] and $\Delta x$ [Eq. (3.5)]. These positive quantities locate a "starting point" for the problem that determine whether the problem is in a regime described by the thick, intermediate, or thin limits.

This situation is depicted in Fig. 2. The boundaries of the regimes labeled "thick," "intermediate," and "thin" are not precise, but if the starting point lies in the thick regime and the given differencing scheme does not have the thick diffusion limit for the cell-average (or cell-edge) fluxes, then one should not expect accurate cell-average (or cell-edge) fluxes in the resulting numerical solution. A similar statement holds for the intermediate diffusion limit. If the starting point lies in the thin regime, then the truncation error will be small enough that there should be little concern about the accuracy of the numerical solution. Finally, if the starting point lies outside the thick, intermediate, and thin regimes, then the analysis in this article is not relevant.

We wish to emphasize that one cannot make intuitive assumptions regarding a relationship between the thick and intermediate diffusion limits. These limits are

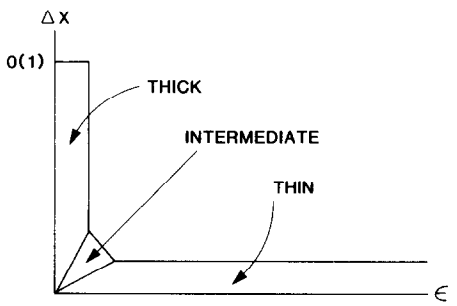


FIG. 2. The thick, intermediate, and thin regimes.

independent, and although the intermediate limit uses many more spatial cells that the thick limit, is not true that a scheme that possesses a thick diffusion limit necessarily possesses an intermediate diffusion limit. In fact, the Lund–Wilson method, treated below, has a thick, but not necessarily an intermediate, diffusion limit. (See Table I) Likewise, we shall analyze several schemes whose cell average fluxes have a particular diffusion limit, but the cell-edge fluxes do not, and it seems possible that a scheme might exist for which the converse could also be true.

In addition, we wish to point out that the concepts of "thick" and "intermediate" diffusion limits have previously been discussed in the literature [19], where they are respectively referred to as "strong" and "weak" asymptotic limits. We use the former choice of words in this article because we believe it is more descriptive.

## IV. The Diamond-Difference Method

The diamond-difference method is a standard method that has been widely used in neutronics codes [10, 11]. It has also been used recently in radiative transfer applications [20]. Here, we study its properties in the thick and intermediate diffusion regimes.

### A. *Thick Regime*

Using Eq. (3.10) in Eq. (3.1), we find that the diamond-difference equations in the thick diffusion regime are

$$\frac{\mu_m}{h_j}(\psi_{m,j+1/2}-\psi_{m,j-1/2})+\frac{\sigma_{Tj}}{\varepsilon}\psi_{mj}=\left(\frac{\sigma_{Tj}}{\varepsilon}-\varepsilon\sigma_{aj}\right)\sum_{n=1}^{N}\psi_{nj}w_n+\varepsilon Q_j, \tag{4.1}$$

$$\psi_{mj}=\tfrac{1}{2}(\psi_{m,j+1/2}+\psi_{m,j-1/2}). \tag{4.2}$$

As in Section II, we introduce the ansatz

$$\psi_m \approx \sum_{k=0}^{\infty}\varepsilon^k\psi_m^{(k)}, \tag{4.3}$$

for both the cell-average and cell-edge fluxes into these equations, equate the coefficients of different powers of $\varepsilon$, and obtain a system of equations that can be solved recursively.

The $O(1/\varepsilon)$ equations are

$$\sigma_{Tj}\left(\psi_{mj}^{(0)}-\sum_{n=1}^{N}\psi_{nj}^{(0)}w_n\right)=0, \tag{4.4}$$

and thus,

$$\psi_{mj}^{(0)}=\phi_j^{(0)}, \tag{4.5}$$

where $\phi_j^{(0)}$ remains to be determined.

The $O(1)$ equations are

$$\sigma_{Tj}\left(\psi_{mj}^{(1)} - \sum_{n=1}^{N} \psi_{nj}^{(1)} w_n\right) = -\frac{\mu_m}{h_j}(\psi_{m,j+1/2}^{(0)} - \psi_{m,j-1/2}^{(0)}), \tag{4.6}$$

$$\psi_{mj}^{(0)} = \tfrac{1}{2}(\psi_{m,j+1/2}^{(0)} + \psi_{m,j-1/2}^{(0)}). \tag{4.7}$$

To analyze these equations, we decompose the cell-edge fluxes into an isotropic and an anisotropic component,

$$\psi_{m,j+1/2}^{(0)} = \phi_{j+1/2}^{(0)} + \eta_{m,j+1/2}^{(0)}, \tag{4.8}$$

with

$$0 = \sum_{n=1}^{N} \eta_{n,j+1/2}^{(0)} w_n. \tag{4.9}$$

Introducing Eqs. (4.5) and (4.8) into (4.7), we obtain

$$\phi_j^{(0)} = \tfrac{1}{2}(\phi_{j+1/2}^{(0)} + \phi_{j-1/2}^{(0)}), \tag{4.10}$$

$$0 = \eta_{m,j+1/2}^{(0)} + \eta_{m,j-1/2}^{(0)}, \tag{4.11}$$

and so

$$\eta_{m,j+1/2}^{(0)} = (-1)^j \eta_m, \tag{4.12}$$

where $\eta_m$ is undetermined. Equation (4.6) now becomes

$$\sigma_{Tj}\left(\psi_{mj}^{(1)} - \sum_{n=1}^{N} \psi_{nj}^{(1)} w_n\right) = -\frac{\mu_m}{h_j}[\phi_{j+1/2}^{(0)} - \phi_{j-1/2}^{(0)} + 2(-1)^j \eta_m], \tag{4.13}$$

and applying the solvability condition (multiplying by $w_m$ and summing over $m$), we obtain

$$0 = \sum_{n=1}^{N} \mu_n \eta_n w_n. \tag{4.14a}$$

We also have, from Eqs. (4.9) and (4.12),

$$0 = \sum_{n=1}^{N} \eta_n w_n. \tag{4.14b}$$

Assuming that these conditions are met, the solution of Eq. (4.13) is

$$\psi_{mj}^{(1)} = \phi_j^{(1)} - \frac{\mu_m}{\sigma_{Tj} h_j}[\phi_{j+1/2}^{(0)} - \phi_{j-1/2}^{(0)} + 2(-1)^j \eta_m]. \tag{4.15}$$

Also,

$$\psi^{(0)}_{m,j+1/2} = \phi^{(0)}_{j+1/2} + (-1)^j \eta_m, \tag{4.16}$$

where the quantities on the right sides of these equations are, at this point, undetermined. [However, $\eta_m$ satisfies the two constraints (4.14).]

The $O(\varepsilon)$ equations in (4.1)–(4.3) are

$$\sigma_{Tj}\left(\psi^{(2)}_{mj} - \sum_{n=1}^{N} \psi^{(2)}_{nj} w_n\right) = -\frac{\mu_m}{h_j}(\psi^{(1)}_{m,j+1/2} - \psi^{(1)}_{m,j-1/2}) - \sigma_{aj}\phi^{(0)}_j + Q_j, \tag{4.17}$$

$$\psi^{(1)}_{mj} = \tfrac{1}{2}(\psi^{(1)}_{m,j+1/2} + \psi^{(1)}_{m,j-1/2}). \tag{4.18}$$

Applying the solvability condition to Eq. (4.17), we get

$$0 = -\sum_{n=1}^{N} \mu_n(\psi^{(1)}_{n,j+1/2} - \psi^{(1)}_{n,j-1/2})\, w_n - (\sigma_a h)_j \phi^{(0)}_j + (hQ)_j. \tag{4.19}$$

Here we have introduced the notation $(\sigma_a h)_j = \sigma_{aj} h_j$, etc. Adding Eq. (4.19) to the corresponding equation for the $(j+1)$st cell and using Eq. (4.18), we obtain

$$\begin{aligned} 0 = &-2\sum_{n=1}^{N} \mu_n(\psi^{(1)}_{n,j+1} - \psi^{(1)}_{n,j})\, w_n \\ &- [(\sigma_a h)_{j+1}\phi^{(0)}_{j+1} + (\sigma_a h)_j \phi^{(0)}_j] + [(hQ)_{j+1} + (hQ)_j]. \end{aligned} \tag{4.20}$$

Finally, introducing Eqs. (4.15) and (4.10) into this result and rearranging, we get

$$\phi^{(0)}_{j+1/2} = \Phi_{j+1/2} + (-1)^{j+1}\left[3\sum_{n=1}^{N} \mu_n^2 \eta_n w_n\right], \tag{4.21}$$

where $\Phi_{j+1/2}$ satisfies the edge-differenced diffusion equation

$$\begin{aligned} &-\left[\frac{1}{3(\sigma_T h)_{j+1}}(\Phi_{j+3/2} - \Phi_{j+1/2}) - \frac{1}{3(\sigma_T h)_j}(\Phi_{j+1/2} - \Phi_{j-1/2})\right] \\ &\quad + \tfrac{1}{4}[(\sigma_a h)_{j+1}(\Phi_{j+3/2} + \Phi_{j+1/2}) + (\sigma_a h)_j(\Phi_{j+1/2} + \Phi_{j-1/2})] \\ &\quad = \tfrac{1}{2}[(hQ)_{j+1} + (hQ)_j]. \end{aligned} \tag{4.22}$$

Equations (4.7), (4.16), and (4.21) now give

$$\psi_{m,j+1/2} = \Phi_{j+1/2} + (-1)^j\left[\eta_m - 3\sum_{n=1}^{N} \mu_n^2 \eta_n w_n\right] + O(\varepsilon), \tag{4.23}$$

$$\psi_{mj} = \tfrac{1}{2}(\Phi_{j+1/2} + \Phi_{j-1/2}) + O(\varepsilon). \tag{4.24}$$

Thus, since $\Phi_{j+1/2}$ satisfies a legitimate discretization of Eq. (2.20), then, from

Eq. (4.24), the diamond-differenced, cell-average fluxes have the thick diffusion limit. However, from Eq. (4.23), the cell-edge fluxes can oscillate from one cell to the next around the correct result, and if so, they do not have the thick diffusion limit. By Eq. (4.21), the scalar component of the cell-edge fluxes can oscillate as well, and if so, it also will not have the thick diffusion limit.

This analysis shows that, although the cell-edge fluxes do not generally have the thick diffusion limit, they do have this limit if $\eta_m = 0$. In practice, we observe that the diamond-differenced cell-edge fluxes do not oscillate much when the incident boundary fluxes on the thick diffusive region are nearly isotropic, but that they do oscillate substantially if these fluxes are highly anisotropic. This observation agrees with Eqs. (4.14) and (4.23), which show that the anisotropy of the cell-edge fluxes is concurrent with their cell-by-cell oscillations. Thus, anisotropic boundary conditions produce a nonzero $\eta_m$, and this produces anisotropic, oscillating, cell-edge fluxes across the entire physical system. We shall discuss these oscillations further in Section VIII.

B. *Intermediate Regime*

The diamond-difference equations in the intermediate diffusion regime are

$$\frac{\mu_m}{\varepsilon h_j}(\psi_{m,j+1/2} - \psi_{m,j-1/2}) + \frac{\sigma_{Tj}}{\varepsilon}\psi_{mj} = \left(\frac{\sigma_{Tj}}{\varepsilon} - \varepsilon\sigma_{aj}\right)\sum_{n=1}^{N}\psi_{nj}w_n + \varepsilon Q_j, \tag{4.25}$$

$$\psi_{mj} = \tfrac{1}{2}(\psi_{m,j+1/2} + \psi_{m,j-1/2}). \tag{4.26}$$

Referring back to Fig. 1, we see that discretized $S_N$ equations that have the intermediate diffusion limit converge, in the limit $\varepsilon \to 0$, to the analytic diffusion equation. Also, we have assumed that the analytic diffusion and transport solutions are smooth with respect to $x$, and that the analytic transport solution is a smooth function of $\varepsilon$ (see the Introduction). Consequently, for the cell-edge and cell-average fluxes in Eqs. (4.25) and (4.26), we shall *hypothesize* the existence of smooth functions $f_m(x, \varepsilon)$ and $g_m(x, \varepsilon)$ such that

$$\psi_{mj} = f_m(x_j, \varepsilon), \tag{4.27a}$$

$$\psi_{m,j+1/2} = g_m(x_{j+1/2}, \varepsilon). \tag{4.27b}$$

This ansatz need not, in general, be true. In particular, it *a priori* disallows any possibility of oscillatory solutions such as exist in the thick diffusion regime. However, such solutions are not observed in actual calculations in the intermediate diffusion regime. Moreover, we shall show that the predictions obtained from this ansatz agree with our numerical results. Thus, the succes of this ansatz provides its ultimate justification.

Equation (4.27b) and the assumed smoothness of $g_m$ imply that

$$\psi_{m,j\pm1/2} = g_m(x_j, \varepsilon) \pm \frac{\varepsilon h_j}{2}\frac{dg_m}{dx}(x_j, \varepsilon) + \frac{\varepsilon^2 h_j^2}{8}\frac{d^2 g_m}{dx^2}(x_j, \varepsilon) + O(\varepsilon^3), \tag{4.28}$$

and introducing this and Eq. (4.27a) into Eqs. (4.25) and (4.26), we get

$$\mu_m \frac{dg_m}{dx}(x_j, \varepsilon) + \frac{\sigma_{Tj}}{\varepsilon} f_m(x_j, \varepsilon) = \left(\frac{\sigma_{Tj}}{\varepsilon} - \varepsilon\sigma_{aj}\right) \sum_{n=1}^{N} f_n(x_j, \varepsilon)\, w_n + \varepsilon Q_j + O(\varepsilon^2), \tag{4.29}$$

$$f_m(x_j, \varepsilon) = g_m(x_j, \varepsilon) + \frac{\varepsilon^2 h_j^2}{8} \frac{d^2 g_m}{dx^2}(x_j, \varepsilon) + O(\varepsilon^4). \tag{4.30}$$

The second of these equations implies $g_m = f_m + O(\varepsilon^2)$, and hence the first equation can be written

$$\mu_m \frac{df_m}{dx} + \frac{\sigma_T}{\varepsilon} f_m = \left(\frac{\sigma_T}{\varepsilon} - \varepsilon\sigma_a\right) \sum_{n=1}^{N} f_n w_n + \varepsilon Q + O(\varepsilon^2), \tag{4.31}$$

where all quantities are evaluated at $x_j$.

We can now apply the same asymptotic analysis to Eq. (4.31) as we applied earlier to Eq. (2.19). In fact, since the two equations differ only in the $O(\varepsilon^2)$ terms, the results for Eq. (2.19) apply here directly. Thus, there exists a function $\phi^{(0)}(x)$ such that

$$f_m(x, \varepsilon) = \phi^{(0)}(x) + O(\varepsilon), \tag{4.32}$$

where

$$-\frac{d}{dx}\frac{1}{3\sigma_T}\frac{d}{dx}\phi^{(0)} + \sigma_a \phi^{(0)} = Q, \tag{4.33}$$

and where all quantities in these equations are evaluated at $x_j$. Equations (4.27), (4.30), and (4.32) imply

$$\psi_{mj} = \phi^{(0)}(x_j) + O(\varepsilon), \tag{4.34a}$$

$$\psi_{m,j+1/2} = \phi^{(0)}(x_{j+1/2}) + O(\varepsilon). \tag{4.34b}$$

For now, Eq. (4.33) holds just at the points $x_j$, which denote the centers of the spatial cells of an $\varepsilon$-dependent mesh (recall $\Delta x_j = \varepsilon h_j$). However, if we require Eqs. (4.33) and (4.34) to hold for all suitably small $\varepsilon$, and if we recall that $\phi^{(0)}(x)$ must be a smooth function of $x$ because the transport solution is smooth, then we have that Eq. (4.33) must hold for all points $x$ in the physical system. Thus, to leading order, the cell-average and cell-edge fluxes are given by Eqs. (4.34), where $\phi^{(0)}(x)$ satisfies Eq. (4.33) at every point in the system, and so the diamond-differenced cell-edge and cell-average fluxes have the intermediate diffusion limit.

Before concluding this section, we wish to discuss a feature of the intermediate diffusion analysis that we were able to overlook in this treatment of the diamond-difference scheme, but that we cannot overlook in the treatment of other differencing schemes. Specifically, the smoothness assumptions on $f_m(x, \varepsilon)$ and $g_m(x, \varepsilon)$ and Eq. (4.30) imply that there must exist a smooth function $p(x)$ such that

$$h_j = p(x_j). \tag{4.35}$$

(The choice of this function determines how the mesh is refined as $\varepsilon \to 0$. This is discussed in Appendix A.) Therefore, in performing the intermediate diffusion analysis, we must assume that the width of the spatial cells is, itself, a smoothly varying function of position. We indicate in each of the following sections where this assumption becomes necessary, but we state here that we cannot derive any intermediate diffusion results without this assumption; thus, one should regard this assumption as an inherent part of the intermediate diffusion analysis.

The results of this section are summarized in Table I.

## V. The Step Method

Although the diamond-difference method is very popular, it has the drawback of not always producing positive solutions, particularly in problems that are not diffusive. As an alternative, we now consider the "step" differencing scheme [10, 11], which has the virtues of being extremely simple and of always producing positive solutions.

### A. *Thick Regime*

The step equations in the thick diffusion regime are

$$\frac{\mu_m}{h_j}(\psi_{m,j+1/2} - \psi_{m,j-1/2}) + \frac{\sigma_{Tj}}{\varepsilon}\psi_{mj} = \left(\frac{\sigma_{Tj}}{\varepsilon} - \varepsilon\sigma_{aj}\right)\sum_{n=1}^{N}\psi_{nj}w_n + \varepsilon Q_j, \tag{5.1}$$

$$\psi_{mj} = \psi_{m,j\pm 1/2}, \tag{5.2}$$

where here and elsewhere in this article, we take "$\pm$" to mean "$+$" if $\mu_m > 0$, and "$-$" if $\mu_m < 0$. Introducing the ansatz for the cell-edge and cell-average fluxes

$$\psi_m \approx \sum_{k=0}^{\infty} \varepsilon^k \psi_m^{(k)}, \tag{5.3}$$

and equating the coefficients of different powers of $\varepsilon$, we obtain a sequence of equations that can be solved recursively.

The $O(1/\varepsilon)$ equation is

$$\sigma_{Tj}\left(\psi_{mj}^{(0)} - \sum_{n=1}^{N}\psi_{nj}^{(0)}w_n\right) = 0, \tag{5.4}$$

and hence

$$\psi_{mj}^{(0)} = \phi_j^{(0)}, \tag{5.5}$$

where $\phi_j^{(0)}$ remains to be determined.

The $O(1)$ equations are

$$\sigma_{Tj}\left(\psi_{mj}^{(1)} - \sum_{n=1}^{N} \psi_{nj}^{(1)} w_n\right) = -\frac{\mu_m}{h_j}\left(\psi_{m,j+1/2}^{(0)} - \psi_{m,j-1/2}^{(0)}\right), \tag{5.6}$$

$$\psi_{mj}^{(0)} = \psi_{m,j\pm 1/2}^{(0)}. \tag{5.7}$$

Combining the above three equations, we get

$$\sigma_{Tj}\left(\psi_{mj}^{(1)} - \sum_{n=1}^{N} \psi_{nj}^{(1)} w_n\right) = -\frac{\mu_m}{h_j}\left(\phi_{j+1/2\mp 1/2}^{(0)} - \phi_{j-1/2\mp 1/2}^{(0)}\right), \tag{5.8}$$

and applying the solvability condition, we obtain

$$0 = -\frac{1}{h_j}\left(\sum_{\mu_n > 0} \mu_n w_n\right)\left(\phi_{j-1}^{(0)} - 2\phi_j^{(0)} + \phi_{j+1}^{(0)}\right). \tag{5.9}$$

This is a legitimate discretization of the standard diffusion equation only if $Q = \sigma_a = 0$, and $(\sigma_T h)_{j+1/2} = \text{constant}$. Under these very restrictive conditions, the step cell-average fluxes have the thick diffusion limit; otherwise, they do not. Also, since manipulating Eqs. (5.5) and (5.7) yields

$$\psi_{m,j+1/2}^{(0)} = \phi_{j+1/2\mp 1/2}^{(0)}, \tag{5.10}$$

the cell-edge fluxes also have the thick diffusion limit under the same restrictive conditions.

B. *Intermediate Regime*

The step equations in the intermediate diffusion regime are

$$\frac{\mu_m}{\varepsilon h_j}\left(\psi_{m,j+1/2} - \psi_{m,j-1/2}\right) + \frac{\sigma_{Tj}}{\varepsilon}\psi^{mj} = \left(\frac{\sigma_{Tj}}{\varepsilon} - \varepsilon\sigma_{aj}\right)\sum_{n=1}^{N} \psi_{nj} w_n + \varepsilon Q_j, \tag{5.11}$$

$$\psi_{mj} = \psi_{m,j\pm 1/2}. \tag{5.12}$$

As in the previous section, we hypothesize the existence of smooth functions $f_m(x, \varepsilon)$ and $g_m(x, \varepsilon)$ such that Eqs. (4.27) and (4.28) hold. Equations (5.11) and (5.12) then become

$$\mu_m \frac{dg_m}{dx}(x_j, \varepsilon) + \frac{\sigma_{Tj}}{\varepsilon} f_m(x_j, \varepsilon) = \left(\frac{\sigma_{Tj}}{\varepsilon} - \varepsilon\sigma_{aj}\right)\sum_{n=1}^{N} f_n(x_j, \varepsilon) w_n + \varepsilon Q_j + O(\varepsilon^2), \tag{5.13}$$

$$f_m(x_j, \varepsilon) = \left(1 \pm \frac{\varepsilon h_j}{2}\frac{d}{dx}\right) g_m(x_j, \varepsilon) + O(\varepsilon^2). \tag{5.14}$$

For the asymptotic analysis to be consistent with the assumed smoothness of $f_m(x, \varepsilon)$ and $g_m(x, \varepsilon)$, it is necessary that there exist a smooth function $p(x)$ such that

$$h_j = p(x_j). \tag{5.15}$$

(See Appendix A.) Equation (5.14) then implies

$$g_m(x_j, \varepsilon) = \left[1 \mp \frac{\varepsilon}{2} p(x_j) \frac{d}{dx}\right] f_m(x_j, \varepsilon) + O(\varepsilon^2), \tag{5.16}$$

and using this result to eliminate $g_m$ from Eq. (5.13), we obtain

$$\mu_m \frac{d}{dx}\left(1 \mp \frac{\varepsilon p}{2} \frac{d}{dx}\right) f_m + \frac{\sigma_T}{\varepsilon} f_m = \left(\frac{\sigma_T}{\varepsilon} - \varepsilon \sigma_a\right) \sum_{n=1}^{N} f_n w_n + \varepsilon Q + O(\varepsilon^2). \tag{5.17}$$

Now we apply exactly the same asymptotic analysis to this equation as we previously applied to Eqs. (2.19) and (4.31). Omitting the straightforward details, we obtain

$$\psi_{m, j+1/2} = \phi^{(0)}(x_{j+1/2}) + O(\varepsilon), \tag{5.18a}$$

$$\psi_{mj} = \phi^{(0)}(x_j) + O(\varepsilon), \tag{5.18b}$$

where

$$-\frac{d}{dx}\left(\frac{1}{3\sigma_T} + \alpha\right) \frac{d\phi^{(0)}}{dx} + \sigma_a \phi^{(0)} = Q, \tag{5.19}$$

and

$$\alpha(x) = p(x) \sum_{\mu_m > 0} \mu_m w_m. \tag{5.20}$$

These equations imply that the step cell-average and cell-edge fluxes do not possess the intermediate diffusion limit unless $Q_j = \sigma_{aj} = 0$, $\sigma_{Tj} =$ constant, and $h_j =$ constant.

The results of this section are summarized in Table I.

## VI. The Lund–Wilson and Castor Methods

The Lund–Wilson [12, 13] and Castor [14] methods are modifications of the step method, and are designed to give better cell-average fluxes than the step method for spatial meshes that are not optically thin. In dimensional quantities, these methods are defined by the balance equation

$$\frac{\mu_m}{\Delta z_j}(\tilde{\psi}_{m, j+1/2} - \tilde{\psi}_{m, j-1/2}) + \tilde{\sigma}_{Tj} \tilde{\psi}_{mj} = \tilde{\sigma}_s \sum_{n=1}^{N} \tilde{\psi}_{nj} w_n + \tilde{Q}_j, \tag{6.1}$$

and the auxiliarry equations

$$\tilde{\psi}_{mj} = \tilde{\gamma}_{m,j\pm 1/2}\tilde{\psi}_{m,j\pm 1/2}, \tag{6.2}$$

$$\tilde{\gamma}_{m,j+1/2} = \begin{cases} 1 + \tilde{\tau}_{m,j+1/2} & \text{(Lund–Wilson)}, \\ \dfrac{\tilde{\tau}_{m,j+1/2}}{2} + \sqrt{1 + \left(\dfrac{\tilde{\tau}_{m,j+1/2}}{2}\right)^2} & \text{(Castor)}, \end{cases} \tag{6.3}$$

$$\tilde{\tau}_{m,j+1/2} = \frac{(\tilde{\sigma}_T \Delta z)_{j+1/2}}{2|\mu_m|}. \tag{6.4}$$

Here, $(\tilde{\sigma}_T \Delta z)_{j+1/2}$ can be any reasonable definition denoting an optical distance between the "centers" of the $j$th and $(j+1)$st cells. For example, Lund recommends for his method the harmonic mean

$$\frac{1}{(\tilde{\sigma}_T \Delta z)_{j+1/2}} = \frac{1}{2}\left[\frac{1}{(\tilde{\sigma}_T \Delta z)_j} + \frac{1}{(\tilde{\sigma}_T \Delta z)_{j+1}}\right], \tag{6.5}$$

but for our diffusion limit analysis, one could equally well choose the arithmetic mean

$$(\tilde{\sigma}_T \Delta z)_{j+1/2} = \tfrac{1}{2}[(\tilde{\sigma}_T \Delta z)_j + (\tilde{\sigma}_T \Delta z)_{j+1}]. \tag{6.6}$$

The Lund–Wilson and Castor methods have the following general properties: they are positive (i.e., they cannot produce a negative angular flux), the cell-average and cell-edge fluxes cannot simultaneously equal the infinite-medium solution $\tilde{\psi} = \tilde{Q}/\tilde{\sigma}_a$, and the truncation error is first order in $\tilde{\sigma}_T \Delta z$ as this quantity tends to zero.

A. *Thick Regime*

In the thick regime, the Lund–Wilson and Castor methods are described by

$$\frac{\mu_m}{h_j}(\psi_{m,j+1/2} - \psi_{m,j-1/2}) + \frac{\sigma_{Tj}}{\varepsilon}\psi_{mj} = \left(\frac{\sigma_{Tj}}{\varepsilon} - \varepsilon\sigma_{aj}\right)\sum_{n=1}^{N}\psi_{nj}w_n + \varepsilon Q_j, \tag{6.7}$$

$$\psi_{mj} = \left[\frac{1}{\varepsilon}\tau_{m,j\pm 1/2} + \beta + O(\varepsilon)\right]\psi_{m,j\pm 1/2}, \tag{6.8}$$

$$\tau_{m,j+1/2} = \frac{(\sigma_T h)_{j+1/2}}{2|\mu_m|}, \tag{6.9}$$

with

$$\beta = \begin{cases} 1 & \text{(Lund–Wilson)} \\ 0 & \text{(Castor)}. \end{cases} \tag{6.10}$$

We introduce the ansatz

$$\psi_m \approx \sum_{k=0}^{\infty} \varepsilon^k \psi_m^{(k)}, \tag{6.11}$$

for both the cell-edge and cell-average fluxes into Eqs. (6.7) and (6.8), equate the coefficients of different powers of $\varepsilon$, and obtain a sequence of equations that can be solved recursively.

The $O(1/\varepsilon)$ equations are

$$\sigma_{Tj}\left(\psi_{mj}^{(0)} - \sum_{n=1}^{N} \psi_{nj}^{(0)} w_n\right) = 0, \tag{6.12}$$

$$0 = \tau_{m,j\pm 1/2} \psi_{m,j\pm 1/2}^{(0)}, \tag{6.13}$$

which yield

$$\psi_{mj}^{(0)} = \phi_j^{(0)}, \tag{6.14}$$

$$\psi_{m,j+1/2}^{(0)} = 0, \tag{6.15}$$

where $\phi_j^{(0)}$ is undetermined. Since the leading-order components of the cell-edge fluxes are zero, we see immediately that these fluxes cannot have the thick diffusion limit.

The $O(1)$ equations are, using the above results,

$$\sigma_{Tj}\left(\psi_{mj}^{(1)} - \sum_{n=1}^{N} \psi_{nj}^{(1)} w_n\right) = 0, \tag{6.16}$$

$$\phi_j^{(0)} = \tau_{m,j\pm 1/2} \psi_{m,j\pm 1/2}^{(1)}, \tag{6.17}$$

which yield

$$\psi_{mj}^{(1)} = \phi_j^{(1)}, \tag{6.18}$$

$$\psi_{m,j+1/2}^{(1)} = \frac{1}{\tau_{m,j+1/2}} \phi_{j+1/2\,1/2}^{(0)}, \tag{6.19}$$

where $\phi_j^{(1)}$ is undetermined.

The $O(\varepsilon)$ equation arising from Eq. (6.7) is

$$\sigma_T\left(\psi_{mj}^{(2)} - \sum_{n=1}^{N} \psi_{nj}^{(2)} w_n\right) = -\frac{\mu_m}{h_j}\left(\psi_{m,j+1/2}^{(1)} - \psi_{m,j-1/2}^{(1)}\right) - \sigma_{aj}\phi_j^{(0)} + Q_j. \tag{6.20}$$

Applying the solvability condition to this equation and using Eq. (6.19), we obtain

$$-\left[\frac{\phi_{j+1}^{(0)} - \phi_j^{(0)}}{3(\sigma_T h)_{j+1/2}} - \frac{\phi_j^{(0)} - \phi_{j-1}^{(0)}}{3(\sigma_T h)_{j-1/2}}\right] + (\sigma_a h)_j\, \phi_j^{(0)} = (hQ)_j. \tag{6.21}$$

This result, together with Eq. (6.14), shows that the Lund–Wilson and Castor cell-average fluxes have the thick diffusion limit.

B. *Intermediate Regime*

The Lund–Wilson and Castor equations in the intermediate diffusion regime can be written

$$\frac{\mu_m}{\varepsilon h_j}(\psi_{m,j+1/2}-\psi_{m,j-1/2})+\frac{\sigma_{Tj}}{\varepsilon}\psi_{mj}=\left(\frac{\sigma_{Tj}}{\varepsilon}-\varepsilon\sigma_{aj}\right)\sum_{n=1}^{N}\psi_{nj}w_n+\varepsilon Q_j, \tag{6.22}$$

$$\psi_{mj}=\gamma_{m,j\pm1/2}\psi_{m,j\pm1/2}, \tag{6.23}$$

$$\gamma_{m,j+1/2}=\begin{cases}1+\tau_{m,j+1/2} & \text{(Lund–Wilson)}, \quad (6.24a)\\ \dfrac{\tau_{m,j+1/2}}{2}+\sqrt{1+\left(\dfrac{\tau_{m,j+1/2}}{2}\right)^2} & \text{(Castor)}, \quad (6.24b)\end{cases}$$

with $\tau_{m,j+1/2}$ defined by Eq. (6.9).

As before, we hypothesize the existence of smooth functions $f_m(x,\varepsilon)$ and $g_m(x,\varepsilon)$ such that Eqs. (4.27) and (4.28) hold. Equation (6.23) then gives

$$f_m(x_j,\varepsilon)=\gamma_{m,j\pm1/2}g_m(x_{j\pm1/2},\varepsilon), \tag{6.25}$$

and the smoothness assumptions on $f_m$ and $g_m$ are consistent with this equation only if [by Eqs. (6.9) and (6.24)] $(\sigma_T h)_{j+1/2}$ varies smoothly from cell to cell. To meet this condition, we assume that there exists a smooth function $p(x)$ such that

$$h_j=p(x_j). \tag{6.26}$$

(See Appendix A) Also, we have assumed that $\sigma_T(x)$ is a smooth function of $x$; and, thus, we may write

$$\sigma_{Tj}=s(x_j,\varepsilon). \tag{6.27}$$

[For example, if $\sigma_{Tj}$ is the average value of $\sigma_T(x)$ in a cell, then

$$s(x,\varepsilon)=\frac{1}{\varepsilon p(x)}\int_{x-\varepsilon/2\,p(x)}^{x+\varepsilon/2\,p(x)}\sigma_T(x')\,dx'.\Big] \tag{6.28}$$

Using Eqs. (6.26) and (6.27) in the definition of $(\sigma_T h)_{j+1/2}$ being used [see, for example, Eqs. (6.5) and (6.6)], we get

$$(\sigma_T h)_{j+1/2}=r(x_{j+1/2},\varepsilon), \tag{6.29}$$

where $r(x,\varepsilon)$ is a smooth function of $x$ and $\varepsilon$, and the dependence on $\varepsilon$ occurs because of the (possible) dependence of $s$ on $\varepsilon$.

Now, by Eqs. (6.24), we may write

$$\gamma_{m,j+1/2}=\Gamma(\tau_{m,j+1/2}), \tag{6.30}$$

where $\Gamma(\tau)$ is a smooth function of $\tau$, defined differently for the two methods. If we define

$$\xi_m(x, \varepsilon) = \Gamma\left[\frac{r(x, \varepsilon)}{2|\mu_m|}\right], \tag{6.31}$$

then $\xi_m$ is a smooth function of $x$ and $\varepsilon$, and

$$\gamma_{m,j+1/2} = \xi_m(x_{j+1/2}, \varepsilon). \tag{6.32}$$

Hence,

$$\gamma_{m,j+1/2} = \xi_m(x_j, \varepsilon) + \frac{\varepsilon p(x_j)}{2}\frac{d\xi_m}{dx}(x_j, \varepsilon) + O(\varepsilon^2). \tag{6.33}$$

Introducing these results into Eqs. (6.22) and (6.23), we obtain

$$\mu_m \frac{dg_m}{dx}(x_j, \varepsilon) + \frac{\sigma_{Tj}}{\varepsilon} f_m(x_j, \varepsilon) = \left(\frac{\sigma_{Tj}}{\varepsilon} - \varepsilon\sigma_{aj}\right) \sum_{n=1}^{N} f_n(x_j, \varepsilon)\, w_n + \varepsilon Q_j + O(\varepsilon^2), \tag{6.34}$$

$$f_m(x_j, \varepsilon) = \left[\xi_m(x_j, \varepsilon) \pm \frac{\varepsilon p(x_j)}{2}\frac{d\xi_m}{dx}(x_j, \varepsilon)\right] \times \left[g_m(x_j, \varepsilon) \pm \frac{\varepsilon p(x_j)}{2}\frac{dg_m}{dx}(x_j, \varepsilon)\right] + O(\varepsilon^2). \tag{6.35}$$

The second of these equations gives

$$g_m(x_j, \varepsilon) = \left\{1 \mp \frac{\varepsilon p(x_j)}{2}\left[\frac{(d\xi_m/dx)(x_j, \varepsilon)}{\xi_m(x_j, \varepsilon)} + \frac{d}{dx}\right]\right\}\frac{f_m(x_j, \varepsilon)}{\xi_m(x_j, \varepsilon)} + O(\varepsilon^2), \tag{6.36}$$

and introducing this result into the first equation, we obtain

$$\mu_m \frac{d}{dx}\left[1 \mp \frac{\varepsilon p}{2}\left(\frac{d\xi_m/dx}{\xi_m} + \frac{d}{dx}\right)\right]\frac{f_m}{\xi_m} + \frac{\sigma_T}{\varepsilon} f_m = \left(\frac{\sigma_T}{\varepsilon} - \varepsilon\sigma_a\right) \sum_{n=1}^{N} f_n w_n + \varepsilon Q + O(\varepsilon^2), \tag{6.37}$$

where all quantities are evaluated at $x_j$.

Now we apply exactly the same asymptotic analysis to this equation as we previously applied to Eqs. (2.19), (4.31), and (5.16). Omitting the straightforward, but somewhat lengthy details, we obtain

$$\psi_{m,j+1/2} = \frac{\phi^{(0)}(x_{j+1/2})}{\gamma_{m,j+1/2}} + O(\varepsilon), \tag{6.38a}$$

$$\psi_{mj} = \phi^{(0)}(x_j) + O(\varepsilon), \tag{6.38b}$$

where $\phi^{(0)}(x)$ satisfies

$$-\frac{d}{dx}\frac{1}{3\sigma_T}\left(u\frac{d}{dx}+v\right)\phi^{(0)}+\sigma_a\,\phi^{(0)}=Q, \tag{6.39}$$

and

$$u(x)=3\sum_{n=1}^{N}\mu_n^2\left[\frac{1+\xi_n(x,0)\,\tau_n(x,0)}{\xi_n^2(x,0)}\right]w_n, \tag{6.40}$$

$$v(x)=\frac{3}{2}\frac{d}{dx}\sum_{n=1}^{N}\frac{\mu_n^2}{\xi_n^2(x,0)}\,w_n, \tag{6.41}$$

$$\tau_m(x,0)=\frac{r(x,0)}{2|\mu_m|}. \tag{6.42}$$

Equation (6.39) is the correct diffusion equation only if $u=1$ and $v=0$. However, by Eqs, (6.41), (6.31), and (6.29), $v=0$ only if $(\sigma_T h)_{j+1/2}$ is independent of $j$. For the Lund–Wilson method, Eqs. (6.24a) and (6.40) give

$$u(x)=3\sum_{n=1}^{N}\mu_n^2\left[\frac{1+\tau_n(x,0)+\tau_n^2(x,0)}{1+2\tau_n(x,0)+\tau_n^2(x,0)}\right]w_n, \tag{6.43}$$

so for finite, nonzero $\sigma_T h$, $u<1$. For Castor's method, however, $\xi_m$ satisfies

$$1+\xi_m\tau_m=\xi_m^2, \tag{6.44}$$

and, thus, by Eq. (6.40), $u=1$.

On the basis of these results and Eqs. (6.38), we can assert the following. Castor's cell-average fluxes have the intermediate diffusion limit only if $(\sigma_T h)_{j+1/2}$ is independent of $j$, and under no circumstances do Castor's cell-edge fluxes have this limit. The Lund–Wilson cell-average fluxes have the intermediate diffusion limit only if $\sigma_{aj}=Q_j=0$ and $(\sigma_T h)_{j+1/2}$ is independent of $j$, and under no circumstances do the Lund–Wilson cell edge fluxes have this limit. These results are summarized in Table I.

## VII. New Method

The following new method possesses all four diffusion limits. In dimensional quantities, it is defined by the balance equation

$$\frac{\mu_m}{\Delta z_j}(\tilde{\psi}_{m,j+1/2}-\tilde{\psi}_{m,j-1/2})+\tilde{\sigma}_{Tj}\tilde{\psi}_{mj}=\tilde{\sigma}_{sj}\sum_{n=1}^{N}\tilde{\psi}_{nj}w_n+\tilde{Q}_j, \tag{7.1}$$

and the auxiliary equations

$$\tilde{\psi}_{mj} = \tilde{\gamma}_{mj}\tilde{\psi}_{m,j\pm 1/2} + (1-\tilde{\gamma}_{mj})\frac{\tilde{\sigma}_{sj}\tilde{\zeta}_{j\pm 1/2} + \tilde{Q}_j}{\sigma_{Tj}}, \tag{7.2}$$

$$\tilde{\gamma}_{mj} = 1 + \frac{(\tilde{\sigma}_T\,\Delta z)_j}{2|\mu_m|}, \tag{7.3}$$

$$\tilde{\zeta}_{j+1/2} = \frac{(\tilde{\sigma}_T\,\Delta z)_{j+1}\sum_{n=1}^{N}\tilde{\psi}_{nj}w_n + (\tilde{\sigma}\,\Delta z)_j\sum_{n=1}^{N}\tilde{\psi}_{n,j+1}w_n}{(\tilde{\sigma}_T\,\Delta z)_{j+1} + (\tilde{\sigma}_T\,\Delta z)_j}. \tag{7.4}$$

This method can easily be shown to have a truncation error that is $O(\tilde{\sigma}_T\,\Delta z)^2$ as $\tilde{\sigma}_T\,\Delta z$ tends to zero, and its cell-edge and cell-average fluxes both possess the infinite-medium solution $\tilde{\psi} = \tilde{Q}/\tilde{\sigma}_a$. [The Lund-Wilson and Castor methods have first-order truncation errors in $\tilde{\sigma}_T\,\Delta z$, and their cell-edge fluxes do not possess the infinite medium solution.] On the other hand, the new method is not strictly positive, whereas the Lund–Wilson and Castor methods are positive.

A. *Thick Regime*

In the thick diffusion regime, the dimensionless, scaled equations become

$$\frac{\mu_m}{h_j}(\psi_{m,j+1/2} - \psi_{m,j-1/2}) + \frac{\sigma_{Tj}}{\varepsilon}\psi_{mj} = \left(\frac{\sigma_{Tj}}{\varepsilon} - \varepsilon\sigma_{aj}\right)\sum_{n=1}^{N}\psi_{nj}w_n + \varepsilon Q_j, \tag{7.5}$$

$$\psi_{mj} = \left(1 + \frac{\tau_{mj}}{\varepsilon}\right)\psi_{m,j\pm 1/2} - \left(\frac{\tau_{mj}}{\varepsilon}\right)\left[\left(1 - \varepsilon^2\frac{\sigma_{aj}}{\sigma_{Tj}}\right)\zeta_{j\pm 1/2} + \varepsilon^2\frac{Q_j}{\sigma_T}\right], \tag{7.6}$$

$$\tau_{mj} = \frac{(\sigma_T h)_j}{2|\mu_m|}, \tag{7.7}$$

$$\zeta_{j+1/2} = \frac{(\sigma_T h)_{j+1}\sum_{n=1}^{N}\psi_{nj}w_n + (\sigma_T h)_j\sum_{n=1}^{N}\psi_{n,j+1}w_n}{(\sigma_T h)_{j+1} + (\sigma_T h)_j}. \tag{7.8}$$

Introducing the usual power-series-in-$\varepsilon$ ansatz for the cell-edge and cell-average fluxes, and also for $\zeta_{j+1/2}$, and equating the coefficients of different powers of $\varepsilon$, we obtain a sequence of equations that can be solved recursively.

The $O(1/\varepsilon)$ equations are

$$\sigma_{Tj}\left(\psi_{mj}^{(0)} - \sum_{n=1}^{N}\psi_{nj}^{(0)}w_n\right) = 0, \tag{7.9}$$

$$\tau_{mj}(\psi_{m,j\pm 1/2}^{(0)} - \zeta_{j\pm 1/2}^{(0)}) = 0, \tag{7.10}$$

and hence

$$\psi_{mj}^{(0)} = \phi_j^{(0)}, \tag{7.11}$$

$$\psi_{m,j+1/2}^{(0)} = \zeta_{j+1/2}^{(0)} \tag{7.12}$$

where $\phi_j^{(0)}$ and $\zeta_{j+1/2}^{(0)}$ are, at this point, undetermined.

The $O(1)$ equations from Eqs. (7.5)–(7.8) and (7.11), (7.12) are

$$\sigma_{Tj}\left(\psi_{mj}^{(1)} - \sum_{n=1}^{N} \psi_{nj}^{(1)} w_n\right) = -\frac{\mu_m}{h_j}\left(\zeta_{j+1/2}^{(0)} - \zeta_{j-1/2}^{(0)}\right), \tag{7.13}$$

$$\tau_{mj}\left(\psi_{m,j\pm 1/2}^{(1)} - \zeta_{j\pm 1/2}^{(1)}\right) = \phi_j^{(0)} - \zeta_{j\pm 1/2}^{(0)}, \tag{7.14}$$

$$\zeta_{j+1/2}^{(0)} = \frac{(\sigma_T h)_{j+1}\,\phi_j^{(0)} + (\sigma_T h)_j\,\phi_{j+1}^{(0)}}{(\sigma_T h)_{j+1} + (\sigma_T h)_j}. \tag{7.15}$$

Solving these, we obtain

$$\psi_{mj}^{(1)} = \phi_j^{(1)} - \frac{\mu_m}{(\sigma_T h)_j}\left(\zeta_{j+1/2}^{(0)} - \zeta_{j-1/2}^{(0)}\right), \tag{7.16}$$

$$\psi_{m,j+1/2}^{(1)} = \zeta_{j+1/2}^{(1)} - \frac{\mu_m}{(\sigma_T h)_{j+1/2}}\left(\phi_{j+1}^{(0)} - \phi_j^{(0)}\right), \tag{7.17}$$

where

$$(\sigma_T h)_{j+1/2} = \tfrac{1}{2}\left[(\sigma_T h)_{j+1} + (\sigma_T h)_j\right], \tag{7.18}$$

and where $\phi_j^{(1)}$ and $\zeta_{j+1/2}^{(1)}$ are undetermined.

The $O(\varepsilon)$ part of Eq. (7.5) is

$$\sigma_{Tj}\left[\psi_{mj}^{(2)} - \sum_{n=1}^{N} \psi_{nj}^{(2)} w_n\right] = -\frac{\mu_m}{h_j}\left(\psi_{m,j+1/2}^{(1)} - \psi_{m,j-1/2}^{(1)}\right) - \sigma_{aj}\,\phi_j^{(0)} + Q_j. \tag{7.19}$$

Applying the solvability condition and using Eq. (7.17), we get

$$-\left[\frac{\phi_{j+1}^{(0)} - \phi_j^{(0)}}{3(\sigma_T h)_{j+1/2}} - \frac{\phi_j^{(0)} - \phi_{j-1}^{(0)}}{3(\sigma_T h)_{j-1/2}}\right] + (\sigma_a h)_j\,\phi_j^{(0)} = (hQ)_j. \tag{7.20}$$

Thus, from Eqs. (7.11), (7.12), (7.15), and (7.20), the cell-average and cell-edge fluxes have the thick diffusion limit.

## B. *Intermediate Regime*

In the intermediate diffusion limit, the dimensionless equations become

$$\frac{\mu_m}{\varepsilon h_j}\left(\psi_{m,j+1/2} - \psi_{m,j-1/2}\right) + \frac{\sigma_{Tj}}{\varepsilon}\psi_{mj} = \left(\frac{\sigma_{Tj}}{\varepsilon} - \varepsilon\sigma_{aj}\right)\sum_{n=1}^{N} \psi_{nj} w_n + \varepsilon Q_j, \tag{7.21}$$

$$\psi_{mj} = (1 + \tau_{mj})\,\psi_{m,j\pm 1/2} - \tau_{mj}\left[\left(1 - \varepsilon^2\frac{\sigma_{aj}}{\sigma_{Tj}}\right)\zeta_{j\pm 1/2} + \varepsilon^2\frac{Q_j}{\sigma_{Tj}}\right], \tag{7.22}$$

$$\zeta_{j+1/2} = \frac{(\sigma_T h)_{j+1}\sum_{n=1}^{N}\psi_{nj} w_n + (\sigma_T h)_j \sum_{n=1}^{N}\psi_{n,j+1} w_n}{(\sigma_T h)_{j+1} + (\sigma_T h)_j}, \tag{7.23}$$

with $\tau_{mj}$ defined by Eq. (7.7). As in the previous sections, we hypothesize the existence of smooth functions $f_m(x, \varepsilon)$ and $g_m(x, \varepsilon)$ such that Eqs. (4.27) and (4.28) hold. Then, as in the previous sections, we must also hypothesize the existence of smooth function $p(x, \varepsilon)$ and $t(x, \varepsilon)$ such that

$$h_j = p(x_j), \tag{7.24}$$

$$(\sigma_T h)_j = t(x_j, \varepsilon). \tag{7.25}$$

Introducing all these expressions into Eq. (7.23) and expanding about the point $x_j$, we obtain

$$\zeta_{j\pm 1/2} = \sum_{n=1}^{N} f_n(x_j, \varepsilon) \pm \frac{\varepsilon p(x_j)}{2} \sum_{n=1}^{N} \frac{df_n}{dx}(x_j, \varepsilon)\, w_n + O(\varepsilon^2). \tag{7.26}$$

Thus, Eqs. (7.21) and (7.22) become

$$\mu_m \frac{dg_m}{dx} + \frac{\sigma_T}{\varepsilon} f_m = \left(\frac{\sigma_T}{\varepsilon} - \varepsilon\sigma_{aj}\right) \sum_{n=1}^{N} f_n w_n + \varepsilon Q_j + O(\varepsilon^2), \tag{7.27}$$

$$f_m = \left(1 + \frac{t}{2|\mu_m|}\right)\left(g_m \pm \frac{\varepsilon p}{2}\frac{dg_m}{dx}\right) - \frac{t}{2|\mu_m|}\left[\sum_{n=1}^{N} f_n w_n \pm \frac{\varepsilon p}{2} \sum_{n=1}^{N} \frac{df_n}{dx} w_n\right] + O(\varepsilon^2). \tag{7.28}$$

At this point, it is algebraically simplest to adopt a somewhat different procedure than in the previous sections. Namely, we expand *both* $f_m$ and $g_m$ in a power series in $\varepsilon$,

$$f_m(x, \varepsilon) \approx \sum_{k=0}^{\infty} \varepsilon^k f_m^{(k)}(x), \tag{7.29a}$$

$$g_m(x, \varepsilon) \approx \sum_{k=0}^{\infty} \varepsilon^k g_m^{(k)}(x), \tag{7.29b}$$

and we introduce these series into Eqs. (7.27) and (7.28), equate the coefficients of different powers of $\varepsilon$, and obtain a sequence of equations that can be solved recursively. The details are straightforward, and we omit them. Using the fact that as $\varepsilon \to 0$, Eqs. (7.24) and (7.25) give

$$\sigma_T(x)\, p(x) = t(x, 0), \tag{7.30}$$

we obtain

$$\psi_{mj} = \phi^{(0)}(x_j) + O(\varepsilon), \tag{7.31}$$

$$\psi_{m,j+1/2} = \phi^{(0)}(x_{j+1/2}) + O(\varepsilon), \tag{7.32}$$

where

$$-\frac{d}{dx}\frac{1}{3\sigma_T}\frac{d}{dx}\phi^{(0)}+\sigma_a\phi^{(0)}=Q; \tag{7.33}$$

therefore, the cell-average and cell-edge fluxes have the intermediate diffusion limit.

Thus, as shown in Table I, this new differencing scheme has all four diffusion limits. It is relatively straightforward to generalize this scheme to produce additional schemes that also have all four diffusion limits. One such differencing scheme, which is more complicated than the scheme presented here, but which is more positive, is described in [19].

## VIII. Numerical Results

In this section, we describe numerical results for five problems chosen to test the theoretical predictions made in the previous sections. We describe each problem with its numerical results separately, and then we give a brief summary. All of the following problems used the standard $S_8$ Gauss–Legendre quadrature set, and all of the "exact" solutions were obtained using the diamond-difference method with $10^4$ equal spatial cells. In addition, we refer to the various spatial meshes as either "intermediate" or "thick" to indicate the asymptotic regimes within which the discretizations lie.

*Problem* 1

$$\mu_m\frac{d\psi_m}{dz}+100\,\psi_m=100\sum_{n=1}^{N}\psi_n w_n+0.01, \qquad 0<z<10,$$

$$\psi_m(0)=0, \qquad \mu_m>0,$$

$$\psi_m(10)=0, \qquad \mu_m<0,$$

$$\Delta z=\begin{cases}1.0 & \text{(thick)}\\ 0.01 & \text{(intermediate).}\end{cases}$$

In Figs. 3–6, we display the cell-average and edge scalar fluxes for the thick and intermediate spatial differencings. (In these and all subsequent figures, we use the abbreviations DD = diamond difference, SD = step difference, LW = Lund–Wilson, CD = Castor difference, and ND = new difference scheme.) The results shown in these figures agree with the theoretical predictions. In Fig. 3, the LW and CD

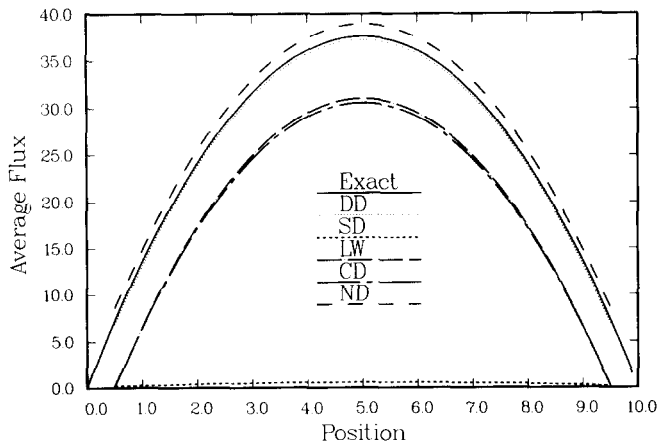


FIG. 3. Problem 1 cell average scalar fluxes: Thick differencing.

solutions are parabolic in shape and, thus, represent a numerical solution of the correct diffusion equation—but with slightly incorrect boundary conditions. This occurs because, at a system boundary, the methods reduce to SD (which does not have the diffusion limit) for the outgoing directions. [In these and all other LW and CD calculations, we used the definition (6.5) for $(\sigma_T h)_{j+1/2}$, which, with $\sigma_T = 0$ outside the system, yields $\sigma_{T,1/2} = \sigma_{T,J+1/2} = 0.$] If we had added two very thin cells, one at each edge of the system, the LW and CD solutions would have been much more accurate.

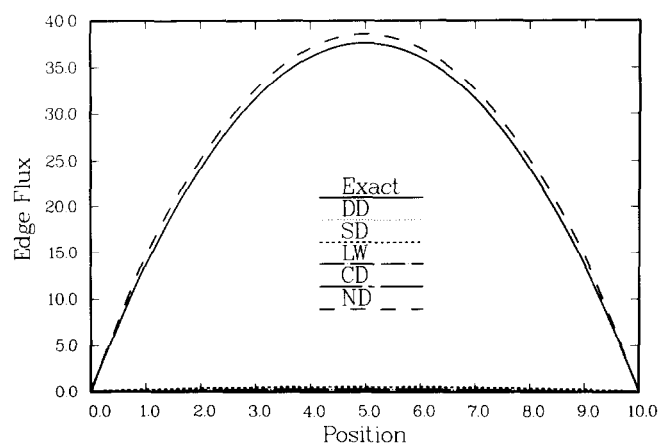


FIG. 4. Problem 1 cell edge scalar fluxes: Thick differencing. (The DD and exact curves are coincident, and the SD, LW, and CD curves are essentially zero.)

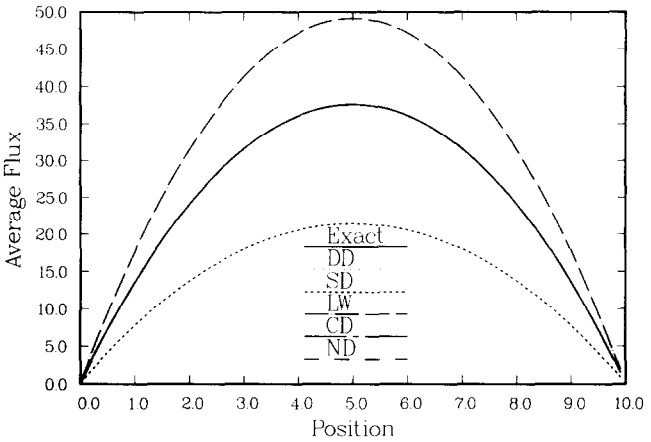


FIG. 5. Problem 1 cell average scalar fluxes: Intermediate differencing. (The exact, DD, CD, and ND curves are coincident.)

*Problem* 2

$$\mu_m \frac{d\psi_m}{dz} + 100\,\psi_m = 100 \sum_{n=1}^{N} \psi_n w_n, \qquad 0 < z < 10,$$

$$\psi_m(0) = 0, \qquad \mu_m > 0,$$

$$\psi_m(10) = 1.0, \qquad \mu_m < 0,$$

$$\Delta z = \begin{cases} 1.0 & \text{(thick)} \\ 0.01 & \text{(intermediate).} \end{cases}$$

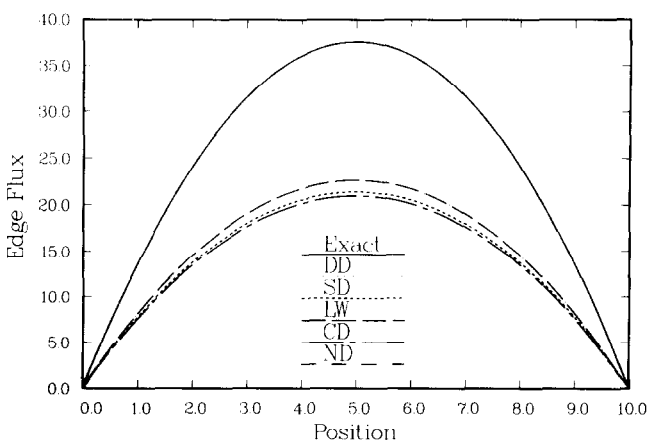


FIG. 6. Problem 1 cell edge scalar fluxes: Intermediate differencing. (The exact, DD, and ND curves are coincident.)

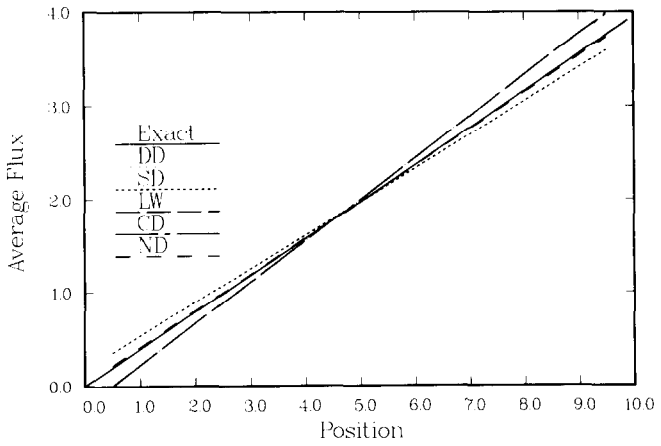


FIG. 7. Problem 2 cell average scalar fluxes: Thick differencing. (The exact, DD, SD, and ND curves are coincident.)

Here we give two Figs., 7 and 8, displaying the cell-average fluxes for the thick and intermediate spatial differencings. Now, all of the methods have both diffusion limits (i.e., all of the solutions have the correct linear shape, which agrees with our theory). However, as with the previous problem, the LW and CD solutions have somewhat incorrect boundary values, which lead to inaccuracies within the system, and these inaccuracies are greater with the intermediate spatial differencing.

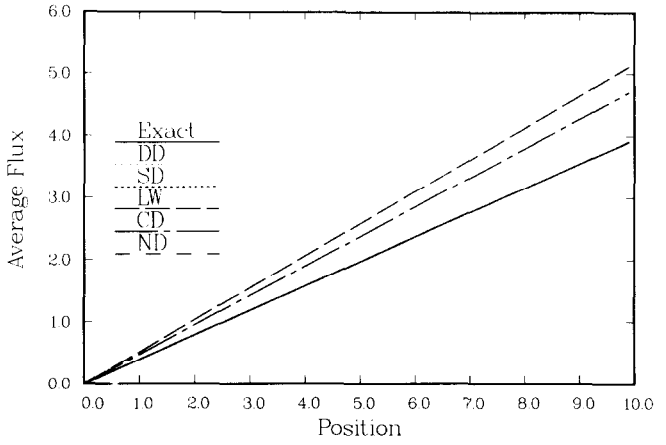


FIG. 8. Problem 2 cell average scalar fluxes: Intermediate differencing. (The exact and DD curves are coincident; the LW and CD curves are coincident.)

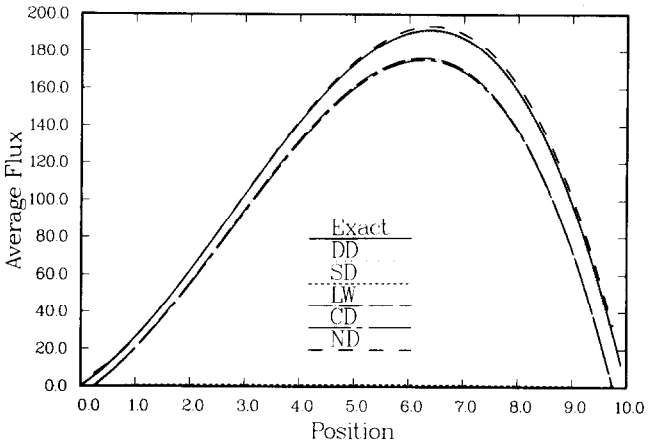


FIG. 9. Problem 3 cell average scalar fluxes: Thick differencing.

*Problem* 3

$$\mu_m \frac{d\psi_m}{dz} + 100(1+z)\,\psi_m = 100(1+z)\sum_{n=1}^{N} \psi_n w_n + 0.01, \qquad 0 < z < 10,$$

$$\psi_m(0) = 0, \qquad \mu_m > 0,$$

$$\psi_m(10) = 0, \qquad \mu_m < 0,$$

$$\Delta z = \begin{cases} 0.5 & \text{(thick)} \\ 0.005 & \text{(intermediate)}. \end{cases}$$

This problem was chosen to test the theoretical predictions for non-constant $\tilde{\sigma}_T\,\Delta z$; in the thick differencing $\tilde{\sigma}_T\,\Delta z$ monotonically varies from 62.5 to 537.5,

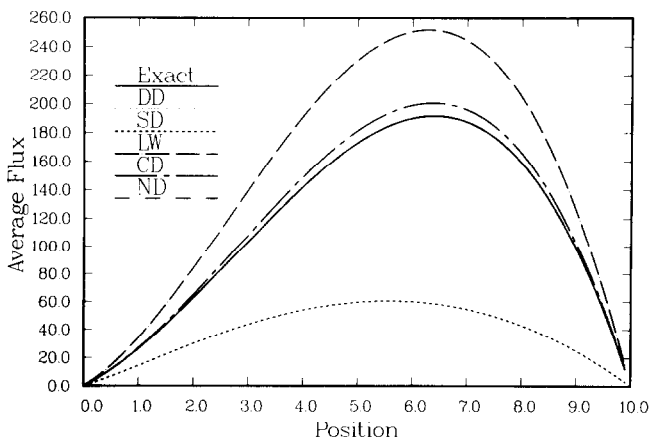


FIG. 10. Problem 3 cell average scalar fluxes: Intermediate differencing. (The exact, DD, and ND curves are coincident.)

while in the intermediate differencing, the variation is from 0.625 to 5.375. In Figs. 9 and 10, the cell-average fluxes are plotted for the thick and intermediate spatial meshes, and as with the previous problems, these results agree with our theory. The [redacted] seness of the cells at the system boundaries. Also, the intermediate CD fluxes are, as predicted, not in agreement with the exact solution, although for this problem, the deviation is not large.

*Problem* 4

$$\mu_m \frac{d\psi_m}{dz} + 100\,\psi_m = 100 \sum_{n=1}^{N} \psi_n w_n, \qquad 0 < z < 10,$$

$$\psi_m(0) = 0, \qquad \mu_m > 0,$$

$$\psi_m(10) = \frac{\delta_{m1}}{w_1}, \qquad \mu_m < 0,$$

$$\Delta z = 1.0 \qquad \text{(thick)}.$$

Here, we order the quadrature set in increasing values of $\mu$, so that $\mu_1$ is the element closest to $-1.0$. Therefore, this problem is driven by a "pencil" beam incident on the right edge of the system in a nearly normal direction. The structure of the exact angular flux is as follows: a transport region or boundary layer, a few mean free paths thick, exists at the right edge of the system, within which the angular flux transitions from a highly anisotropic distribution (at $z = 10$) to a nearly isotropic distribution (a few mean free paths to the left of $z = 10$); in the remainder of the system, the angular flux is nearly isotropic and is well-approximated by diffusion theory.

We include this problem for two reasons. First, the previous problems we have considered involve isotropic boundary conditions; since the leading order term in the asymptotic expansion of the analytic transport equation is itself isotropic, this term in these problems does not contain a boundary layer. However, in this problem, this term does contain a boundary layer, a few (say, five) mean free paths thick. Then, the diffusive region for this problem is (approximately) $0 \leqslant z \leqslant 9.95$, while the boundary layer is (approximately) $9.95 \leqslant z \leqslant 10.0$. Since each spatial cell has width $\Delta z = 1.0$ ( = 100 mean free paths), it is clear that this mesh cannot resolve the rapid variation in $\psi_m$ within the boundary layer. Thus, even though the problem is physically dominated by the diffusive region, the $O(1)$ variations of $\psi_m$ in the boundary layer and the absence of resolution of these variations by the spatial mesh imply that any numerical scheme, even one with all the correct diffusion limits, can give very poor results. We include this problem partly to emphasize this crucial point.

The second reason for including this problem is to demonstrate that the DD scheme does exhibit oscillatory behaviour in the cell-edge fluxes when the boundary source for an optically thick cell is not isotropic. (This oscillatory behaviour has been observed elsewhere for nondiffusive problems [21].)

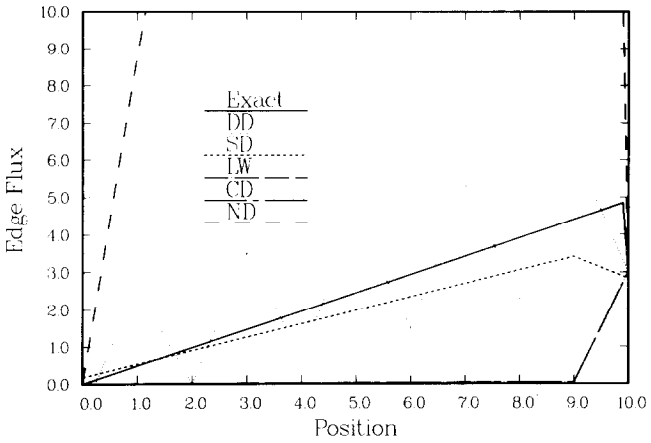


FIG. 11. Problem 4 cell edge scalar fluxes: Thick differencing. (The LW and CD curves are coincident.)

Figure 11 illustrates both these points. Here, the LW and CD edge fluxes are nearly zero, the DD edge fluxes oscillate, and the SD and ND edge fluxes are linear; all this is predicted by theory. [The ND curve rises linearly off the figure from $\phi = 0$ at $z = 0$ to $\phi = 83$ at $z = 9$.] In particular, although the ND cell edge fluxes have the thick diffusion limit and the DD cell-edge fluxes do not, the DD fluxes, even though they exhibit the unphysical oscillation, are more accurate. This is because, for this problem, the lack of resolution of the boundary layer leads to a disastrous value of the ND flux at $z = 9$, and since the ND flux varies linearly (as it should) between $z = 0$ and $z = 9$, the large inaccuracy at $z = 9$ leads to large inaccuracies throughout the system.

Since the DD cell edge fluxes oscillate when the boundary flux for an optically thick cell is not isotropic, and since the presence of such a nonisotropic flux indicates the existence of a boundary layer, one can interpret the presence of oscillating DD cell edge fluxes in a numerical solution as an indication that a boundary layer exists that has not been adequately resolved.

In the next problem, we resolve the above boundary layer and show, among other things, that the oscillations in the DD cell edge fluxes disappear.

*Problem* 5

$$\mu_m \frac{d\psi_m}{dz} + 100\,\psi_m = 100 \sum_{n=1}^{N} \psi_n w_n, \qquad 0 < z < 10,$$

$$\psi_m(0) = 0, \qquad \mu_m > 0,$$

$$\psi_m(10) = \frac{\delta_{m1}}{w_m}, \qquad \mu_m < 0,$$

$$\Delta z = \begin{cases} 0.995 & \text{(first 10 cells; thick)} \\ 0.001 & \text{(last 50 cells; thin)} \end{cases}.$$

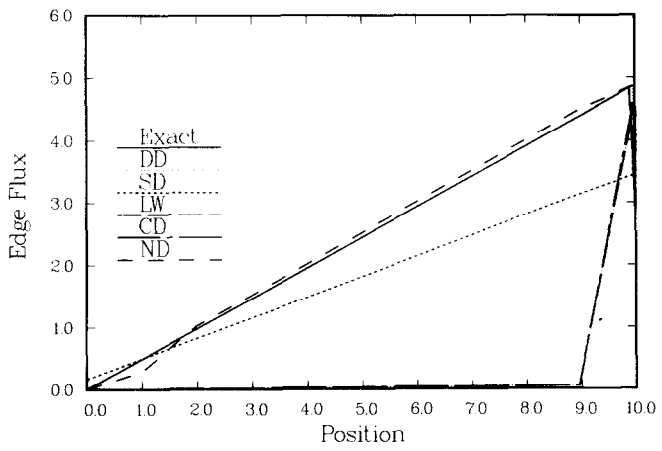


FIG. 12. Problem 5 cell edge scalar fluxes: Thick differencing in diffusive region, thin differencing in boundary layer. (The exact and DD curves are coincident; the LW and CD curves are coincident.)

This is the same physical problem as Problem 4, but now the boundary layer is thoroughly resolved by 50 spatial cells, each 0.1 mean free paths thick, and the diffusive region is differenced with 10 cells, each 99.5 mean free paths thick.

In Fig. 12, we plot the thick cell edge fluxes for this problem. The improvement in the DD and ND results over those in Problem 4 is striking, and is due entirely to the adequate numerical treatment in the boundary layer. The LW and CD fluxes again are nearly zero, as they should be, and the SD solution is linear in the diffusive region, as it should be. The reason why the SD solution is inaccurate is because the mesh is not uniform. In particular, we have $h_9 = h_{10} = 0.995$ and $h_{11} = 0.001$, and so Eq. (5.9) for the $j = 10$ cell does not correspond to a differencing of the correct diffusion equation (in that cell). This shows that even though the SD scheme does give the correct diffusion solution under very special conditions, one cannot violate these conditions and expect to obtain accurate results.

To summarize the numerical results presented above, along with others that we have not included in this article, we can simply state that these results agree with the asymptotic theory. This theory not only predicts when a given differencing scheme does or does not have a given diffusion limit, but it also accurately predicts the manner in which a differencing scheme fails when it does not have a given limit. For example, the LW and CD thick edge fluxes are predicted to vanish, and we observe this in calculations. For another example, in calculations not included in this article, we have numerically solved Eq. (5.19) to verify that the step cell-edge and cell-average intermediate fluxes do satisfy this equation rather than the correct one (with $\alpha = 0$). However, our calculations do emphatically show that the asymptotic theory is valid only for diffusive regions, and that if a differencing scheme has a certain diffusion limit, one can be assured of obtaining good numerical results for the appropriate (edge or average) flux with the appropriate (thick or intermediate) mesh *only* if the nondiffusive regions in the problem are ade-

quately resolved by the spatial mesh. In particular, it is possible for a scheme that does not have a diffusion limit to produce a better result than one that does, if (for the first scheme) the boundary conditions for the diffusive region are sufficiently poor due to an inadequate meshing at a boundary.

## IX. Discussion

In this article, we have considered several spatial differencing schemes for the transport equation and have shown how, in diffusive regions with spatial cells that are not optically thin, one can predict the accuracy of the resulting numerical solutions. Our theoretical tool is an asymptotic expansion that has previously been used to describe the transition from the analytic transport equation to the analytic diffusion equation in "diffusive" problems. We have tested our results numerically and have obtained excellent agreement between theory and experiment. To conclude this article, we briefly consider some additional aspects of our analysis.

First, we discussed in Section III several possible scalings of the dimensionless spatial mesh. The resulting choices,

$$\Delta x_j = \varepsilon^l h_j,$$

with $h_j = O(1)$, $l = 0$ (thick), and $l = 1$ (intermediate), determined the course of the analysis in Sections IV–VII. However, other choices of $l$ are possible and may be of interest. In particular, if $l$ is chosen between 0 and 1, then one has an asymptotic limit "between" the thick and intermediate limits considered above. Since $\varepsilon^l$ appears in Eq. (3.1), the only mathematically workable choices of $l$ are rational, say

$$l = \frac{i}{j},$$

with $i$, $j$ positive integers and $i < j$, and then the ansatz that one would choose for $\psi_m$ would be

$$\psi_m \simeq \sum_{k=0}^{\infty} \varepsilon^{k/j} \psi_m^{(k)}.$$

(Clearly, one would not want to consider values of $j$ that are very large.) Such choices of $l$ lead to curves in Fig. 1 that lie between the intermediate and thick (dashed) lines, and that approach the origin $(\Delta x, \varepsilon) = (0, 0)$ tangent to the vertical axis.

Next, we discuss the concept of "resolving" a solution with a spatial mesh. Roughly, this means that if one knows something about the solution of a given problem and selects a spatial mesh so that the change in the exact solution from one cell to the next is not large, say less than 10%, then the numerical solution ought to be reasonably accurate. (Thus, for example, if a solution has steep gradients, then many cells are required at the location of these gradients, and in

regions where the solution slowly varies, relatively few cells are required.) Moreover, if one has such a mesh and then refines it, the numerical solution should improve. In brief, the familiar concept is that to obtain an accurate numerical solution, it is sufficient to choose a mesh that, in the above sense, "resolves" the exact solution.

The point we wish to make here is that, for transport differencing schemes in diffusive regions, this concept is not always true. One can easily argue that if a scheme has the thick and intermediate limits for the cell-edge and cell-average fluxes, then the concept is valid. However, if this is not the case, then the concept is generally not valid. For example, the step scheme yields an inaccurate solution in Problem 1, even for the intermediate spatial differencing with $10^3$ cells and a very small change in the solution occurring from one cell to the next. Also, the Lund–Wilson cell-average fluxes are reasonably accurate for the thick differencing (10 cells) in Problem 3, but are *less* accurate for the intermediate differencing ($10^3$ cells). The reason for all this, which is not commonly understood, but which we hope is made clear in this article, is that even though the solutions of these problems are $O(1)$ and smooth, the equation that determines the solutions has a small parameter that indicates an underlying singular perturbation problem. Nevertheless, our point remains valid and we repeat: a mesh which "resolves" the diffusion and transport solutions in a diffusive transport problem does not always guarantee an accurate transport approximation. (However, if the mesh is sufficiently resolved so as to be in the thin regime, then the solution will be accurate.)

Also, some of the results in this article could have been obtained by constructing a dispersion law for each transport differencing scheme and then performing the asymptotic expansion on the dispersion law to determine whether a dispersion law for the correct diffusion equation results. Such dispersion laws have found wide use in analyzing the behaviour of very general partial differential equations [22, 23]. However, to construct a dispersion law, one must have an infinite medium with constant cross sections and a uniform mesh, so that the separation of variables technique is workable. Thus, one cannot obtain information regarding the numerical scheme from the dispersion law when the cross sections or the mesh vary. This limitation is not shared by the asymptotic analysis in this article. In particular, our analysis shows that (a) certain differencing schemes have a diffusion limit when $\tilde{\sigma}_T$, $\tilde{\sigma}_s$, and $\Delta z$ vary, and (b) certain schemes have a diffusion limit if $\tilde{\sigma}_T$, $\tilde{\sigma}_s$, and $\Delta z$ are constant, but do not if these quantities vary in a general way. We emphasize that these results could not have been obtained from the analysis of a dispersion law.

In this article we have analyzed spatial differencing schemes that employ two unknowns per cell: the cell-average flux, and the flux on the exiting boundary. There are, however, other schemes that employ three unknowns per cell; such schemes are the linear discontinuous,[24] linear moments,[25] and linear characteristic methods.[24] We have asymptotically analyzed these three schemes in diffusive media, and have found that they possess all four diffusion limits. Details of these results will be presented in a future article.

In addition, in future work we plan to extend the above analysis to curvilinear and multidimensional geometries, and to time- and energy- (or frequency-) dependent problems. We believe that such analyses will successfully predict the accuracy of the corresponding numerical schemes in optically thick, diffusive media.

## APPENDIX A

In this article, we have assumed, for all the intermediate diffusion limit analyses, that we have a spatial mesh with cell edges $x_{j-1/2} < x_{j+1/2}$, with cell centers

$$x_j = \tfrac{1}{2}(x_{j-1/2} + x_{j+1/2}), \tag{(A.1)}$$

and cell widths

$$\Delta x_j = x_{j+1/2} - x_{j-1/2} = \varepsilon p(x_j), \tag{A.2}$$

where $p(x)$ is a smooth function of $x$, independent of $\varepsilon$. In principle, $p(x)$ is selected on the basis of a particular mesh and value of $\varepsilon$, and we wish to use Eqs. (A.1) and (A.2) to define "finer" meshes for smaller values of $\varepsilon$. In this appendix, we prove that, for $p(x)$ sufficiently smooth and $\varepsilon$ sufficiently small, Eqs. (A.1) and (A.2) do, in fact, define a unique set of mesh points $x_j$, $x_{j+1/2}$.

To do this, we note from Eqs. (A.1) and (A.2) that

$$x_{j+1} - x_j = \frac{1}{2}(x_{j+3/2} - x_{j+1/2}) = \frac{\varepsilon}{2}[p(x_{j+1}) + p(x_j)], \tag{A.3}$$

and, thus

$$x_{j+1} - \frac{\varepsilon}{2} p(x_{j+1}) = x_j + \frac{\varepsilon}{2} p(x_j). \tag{A.4}$$

This equation determines the points $x_j$ recursively, with the starting point $x_1$ determined by

$$x_1 = \frac{\varepsilon}{2} p(x_1). \tag{A.5}$$

[Here, we have assumed $x_{1/2} = 0$, and we wish to proceed from left to right across the system.]

We assume that $p(x)$ is continuous, $p'(x)$ is bounded:

$$|p'(x)| < H, \tag{A.6}$$

and we require $\varepsilon$ to be fixed and to satisfy

$$0 < \varepsilon < \frac{2}{H}. \tag{A.7}$$

Then the function

$$F(x) = x - \frac{\varepsilon}{2} p(x), \tag{A.8}$$

satisfies $F'(x) > 0$, and hence is continuous and monotone increasing. Thus, since $F(0) < 0$, exactly one value of $x$ (denoted as $x_1$) exists such that $F(x_1) = 0$. Clearly, $x_1$ satisfies Eq. (A.5).

Next, since $x_1 + (\varepsilon/2)\, p(x_1)$ is positive, exactly one value of $x$ (denoted as $x_2$) exists such that $F(x_2) = x_1 + (\varepsilon/2)\, p(x_1)$. Clearly, $x_2$ satisfies Eq. (A.4) for $j = 1$. In this manner, we recursively determine $x_3$, $x_4$, etc.

Now, having the cell center points $x_j$, we determine the cell edge points recursively by

$$x_{1/2} = 0, \tag{A.9a}$$

$$x_{j+1/2} = x_{j-1/2} + \varepsilon p(x_j). \tag{A.9b}$$

An easy induction proof shows that the points $x_j$ and $x_{j+1/2}$ determined by this process satisfy Eq. (A.1). [They satisfy Eq. (A.2) by virtue of Eq. (A.9).]

Therefore, for $p(x)$ satisfying Eq. (A.6) and all $\varepsilon$ satisfying Eq. (A.7), Eqs. (A.1) and (A.2) define a unique spatial mesh. Moreover, the mesh determined in this way (with a fixed left boundary, $x_{1/2} = 0$) has the property that the cell centers and cell edges depend continuously and monotonically on $\varepsilon$. Therefore, in a finite region [say, $0 \leqslant x \leqslant X$], there are, at most, a countable number of values of $\varepsilon$, descending to zero,

$$0 < \cdots < \varepsilon_3 < \varepsilon_2 < \varepsilon_1,$$

such that cell edges will coincide with $x = X$ as well as $x = 0$. In such a case, one cannot regard the results in this article as holding for "all" $\varepsilon$ sufficiently small, but rather, for all $\varepsilon$ sufficiently small and in this special set.

## Acknowledgments

The authors would like to thank Professors W. L. Filippone and G. C. Pomraning for helpful advice during the preparation of this article. This work was performed under the auspices of the U. S. Department of Energy.

## References

1. J. Pitkaranta, *SIAM J. Numer. Anal.* **15**, 859 (1978).
2. E. W. Larsen and W. F. Miller, Jr., *Nucl. Sci. Eng.* **73**, 76 (1980).
3. E. W. Larsen and P. Nelsen, *SIAM J. Numer. Anal.* **19**, 334 (1982).
4. B. Neta and H. D. Victory, Jr., *SIAM J. Numer. Anal.* **20**, 94 (1983).
5. E. W. Larsen and J. B. Keller, *J. Math. Phys.* **15**, 75 (1974).

6. G. J. HABETLER AND B. J. MATKOWSKY, *J. Math. Phys.* **16**, 846 (1975).
7. G. C. PAPANICOLAOU, *Bull. Am. Math. Soc.* **81**, 330 (1975).
8. E. W. LARSEN, *Ann. Nucl. Energy* **7**, 249 (1980).
9. E. W. LARSEN, G. C. POMRANING, AND V. C. BADHAM, *J. Quant. Spectrosc. Radiat. Transfer* **29**, 285 (1983).
10. B. G. CARLSON AND K. D. LATHROP, in *Computing Methods in Reactor Physics*, edited by H. Greenspan, C. N. Kelber, and D. Okrent (Gordon & Breach, New York, 1968), p. 166.
11. E. E. LEWIS AND W. F. MILLER, JR., *Computational Methods of Neutron Transport* (Wiley–Interscience, New York, 1984).
12. C. M. LUND AND J. R. WILSON, Lawrence Livermore National Laboratory Report No. UCRL-84678, July 1980 (unpublished).
13. C. M. LUND, in *Numerical Astrophysics*, edited by J. Centrella, J. M. LeBlanc, and R. L. Bowers (Jones & Bartlett, Boston 1985), p. 498.
14. J. I. CASTOR, *Comparison of the Errors of the Wilson and Feautrier Schemes for Differencing the Equation of Transfer as Applied to a Class of Simple Model Problems*, Lawrence Livermore National Laboratory Memorandum (Jan. 29, 1982) and Addendum (Feb. 2, 1982).
15. I. P. GRANT, *Mon. Not. R. Astron. Soc.* **125**, 417 (1963).
16. P. A. BROWN, G. R. HILL, AND G. C. POMRANING, *J. Quant. Spectrosc. Radiat. Transfer* **33**, 437 (1985).
17. E. W. LARSEN, *Nucl. Sci. Eng.* **83**, 90 (1983).
18. We use "$S_N$" interchangeably with "discrete-ordinates," even though there is a historical difference between these terms.
19. E. W. LARSEN, J. E. Morel, and W. F. Miller, Jr., *Trans. Am. Nucl. Soc.* 49, 218 (1985).
20. R. E. ALCOUFFE, B. A. CLARK, AND E. W. LARSEN, in *Multiple Time Scales*, edited by J. U. Brackbill and B. Cohen (Academic Press, Orlando, Fla. 1985), p. 73.
21. W. H. REED, *Nucl. Sci. Eng.* **45**, 309 (1971).
22. R. VICHNEVETSKY AND J. B. BOWLES, *Fourier Analysis of Numerical Approximations of Hyperbolic Equations* (Society for Industrial and Applied Mathematics, Philadelphia, 1982).
23. L. N. TREFETHEN, *SIAM Rev.* **24**, 113 (1982).
24. R. E. ALCOUFFE, E. W. LARSEN, W. F. MILLER, JR., AND B. R. WIENKE, Nucl. Sci. Eng. **71**, 111 (1979).
25. R. VAIDYANATHAN, *Nucl. Sci. Eng.* **71**, 46 (1979).